PPAR-δ in *Abca12*$^{-/-}$ keratinocytes (Supplementary Figure S1 online). From our studies and the literature (Di-Poi *et al.*, 2002), PPAR-δ has been shown to have at least an anti-apoptotic role in *Abca12*$^{-/-}$ keratinocytes; however, it remains unclear whether the upregulation of PPAR-δ is in response to apoptosis or decreased ABCA12 expression.

Furthermore, we have measured the mRNA expression levels of other nuclear hormone receptors, including PPAR-α, PPAR-γ, retinoic acid receptor-α, liver X receptor-α, liver X receptor-β, RXR-α, and RXR-γ (Applied Biosystems). The mRNA level of RXR-α from *Abca12*$^{-/-}$ epidermis was shown to be significantly higher than that from wild-type epidermis (Supplementary Figure S1 online). The interaction between the upregulation of RXR-α and AKT activation in keratinocytes has not been reported. However, Wang *et al.* (2011) reported that RXR-α ablation in the epidermis enhances UV-induced apoptosis, which suggests that RXR-α has an anti-apoptotic function in keratinocytes. Thus, upregulation of RXR-α may also have an anti-apoptotic function in *Abca12*$^{-/-}$ keratinocytes.

In conclusion, the present data suggest that keratinocyte apoptosis is involved in the pathomechanisms of HI and that the AKT signaling pathway helps *Abca12*$^{-/-}$ keratinocytes to survive during the keratinization process. In light of this, activation of the AKT signal pathway may be to our knowledge, previously unreported strategy for treating keratinization disorders, including ichthyosis.

CONFLICT OF INTEREST

The authors state no conflict of interest.

ACKNOWLEDGMENTS

We thank Ms Aoyanagi for her technical assistance. This work was supported in part by a grant-in-aid from the Ministry of Education, Science, Sports and Culture of Japan (Kiban A 23249058: to MA), a grant from the Ministry of Health, Labor and Welfare of Japan (Health and Labor Sciences Research Grants; Research on Intractable Disease: H22-177: to MA), and a grant-in-aid from the Japan Society for the Promotion of Science Fellows (to TY).

***Teruki Yanagi*[1], *Masashi Akiyama*[1,2], *Hiroshi Nishihara*[3], *Yuki Miyamura*[1], *Kaori Sakai*[1], *Shinya Tanaka*[4] and *Hiroshi Shimizu*[1]**

[1]Department of Dermatology, Hokkaido University Graduate School of Medicine, Sapporo, Japan; [2]Department of Dermatology, Nagoya University Graduate School of Medicine, Nagoya, Japan; [3]Laboratory of Translational Pathology, Hokkaido University Graduate School of Medicine, Sapporo, Japan and [4]Laboratory of Cancer Research, Department of Pathology, Hokkaido University Graduate School of Medicine, Sapporo, Japan
E-mail: makiyama@med.nagoya-u.ac.jp

SUPPLEMENTARY MATERIAL

Supplementary material is linked to the online version of the paper at http://www.nature.com/jid

REFERENCES

Abe R, Shimizu T, Shibaki A *et al.* (2003) Toxic epidermal necrolysis and Stevens-Johnson syndrome are induced by soluble Fas ligand. *Am J Pathol* 162:1515–20

Akiyama M, Sugiyama-Nakagiri Y, Sakai K *et al.* (2005) Mutations in lipid transporter ABCA12 in harlequin ichthyosis and functional recovery by corrective gene transfer. *J Clin Invest* 115:1777–84

Di-Poi N, Tan NS, Michalik L *et al.* (2002) Antiapoptotic role of PPARbeta in keratinocytes via transcriptional control of the Akt1 signaling pathway. *Mol Cell* 10:721–33

Jiang YJ, Lu B, Kim P *et al.* (2008) PPAR and LXR activators regulate ABCA12 expression in human keratinocytes. *J Invest Dermatol* 128:104–9

Mitsutake S, Suzuki C, Akiyama M *et al.* (2010) ABCA12 dysfunction causes a disorder in glucosylceramide accumulation during keratinocyte differentiation. *J Dermatol Sci* 60:128–9

Moskowitz DG, Fowler AJ, Heyman MB *et al.* (2004) Pathophysiologic basis for growth failure in children with ichthyosis: an evaluation of cutaneous ultrastructure, epidermal permeability barrier function, and energy expenditure. *J Pediatr* 145:82–92

Sun P, Wang XQ, Lopatka K *et al.* (2002) Ganglioside loss promotes survival primarily by activating integrin-linked kinase/Akt without phosphoinositide 3-OH kinase signaling. *J Invest Dermatol* 119:107–17

Thrash BR, Menges CW, Pierce RH *et al.* (2006) AKT1 provides an essential survival signal required for differentiation and stratification of primary human keratinocytes. *J Biol Chem* 281:12155–62

Uchida Y, Houben E, Park K *et al.* (2010) Hydrolytic pathway protects against ceramide-induced apoptosis in keratinocytes exposed to UVB. *J Invest Dermatol* 130: 2472–80

Wang XQ, Sun P, Paller AS (2001) Inhibition of integrin-linked kinase/protein kinase B/Akt signaling: mechanism for ganglioside-induced apoptosis. *J Biol Chem* 276:44504–11

Wang Z, Coleman DJ, Bajaj G *et al.* (2011) RXRalpha ablation in epidermal keratinocytes enhances UVR-induced DNA damage, apoptosis, and proliferation of keratinocytes and melanocytes. *J Invest Dermatol* 131:177–87

Yanagi T, Akiyama M, Nishihara H *et al.* (2008) Harlequin ichthyosis model mouse reveals alveolar collapse and severe fetal skin barrier defects. *Hum Mol Genet* 17:3075–83

Yanagi T, Akiyama M, Nishihara H *et al.* (2010) Self-improvement of keratinocyte differentiation defects during skin maturation in ABCA12-deficient harlequin ichthyosis model mice. *Am J Pathol* 177:106–18

See related commentary on pg 1790

Interpretation of Skindex-29 Scores: Cutoffs for Mild, Moderate, and Severe Impairment of Health-Related Quality of Life

Journal of Investigative Dermatology (2011) **131,** 1945–1947; doi:10.1038/jid.2011.138; published online 19 May 2011

TO THE EDITOR

Health-related quality of life (HRQL) is commonly assessed by means of standardized questionnaires and expressed in domain and overall HRQL scores. An important challenge is to interpret these scores correctly. What does a given score really mean? Although there is no standard approach, several methods exist to facilitate the interpretation of HRQL scores.

In a recently published study (Prinsen *et al.*, 2010), we identified

Abbreviation: HRQL, health-related quality of life

[2] Gudbjartsson DF, Thorvaldsson T, Kong A, Gunnarsson G, Ingolfsdottir A. Allegro version 2. Nat Genet 2005;37:1015–6.
[3] Matise TC, Chen F, Chen W, De La Vega FM, Hansen M, He C, et al. A second-generation combined linkage physical map of the human genome. Genome Res 2007;17:1783–6.

Musharraf Jelani
Muhammad Tariq
Department of Biochemistry, Faculty of Biological Sciences, Quaid-i-Azam University, Islamabad, Pakistan

Iftikhar Ahmad Jan
Hazrat Ullah
Department of Pediatric Surgery, National Institute of Rehabilitation Medicine (NIRM), Islamabad, Pakistan

Muhammad Naeem
Department of Biotechnology, Faculty of Biological Sciences, Quaid-i-Azam University, Islamabad, Pakistan

Wasim Ahmad*
Department of Biochemistry, Faculty of Biological Sciences, Quaid-i-Azam University, Islamabad, Pakistan

*Corresponding author. Tel.: +92 51 90643003; fax: +92 51 9205753
E-mail address: ahmad115@hotmail.com
wahmad@qau.edu.pk (W. Ahmad)

30 June 2010
doi:10.1016/j.jdermsci.2010.11.014

Letter to the Editor

New insight into genotype/phenotype correlations in *ABCA12* mutations in harlequin ichthyosis

Harlequin ichthyosis (HI) is a severe and often fatal congenital ichthyosis with an autosomal recessive inheritance pattern [1]. The clinical features include thick, plate-like scales with ectropion, eclabium and flattened ears. *ABCA12* mutations underlie HI [2,3] and it was clarified that HI is caused by severe functional defects in the keratinocyte lipid transporter ABCA12 [2]. To date, various *ABCA12* mutations have been reported in HI patients [4]. However, genotype/phenotype correlations in *ABCA12* mutations have been poorly elucidated. In order to obtain clues to understand genotype/phenotype correlations in *ABCA12* mutations, we report two HI patients from two independent Japanese families, who were compound heterozygotes for *ABCA12* mutations.

Patient 1 is the second child of healthy, unrelated Japanese parents. The skin of the baby girl was covered with white, diamond shaped plaques at birth (Fig. 1a). After therapy with oral retinoids and local application of white petrolatum, in a humid incubator, the scales gradually detached and passive and spontaneous mobility of the joints increased. Now at the age of 1 year and 7 months, her general condition is good, although she still has white to grey scales on a background of erythematous skin over her entire body. Patient 2 is the fourth child of healthy, unrelated Japanese parents. Her older brother had a history of congenital ichthyosis and died in early infancy. The skin of the newborn showed serious symptoms with thick, white, diamond shaped plaques, partly bordered by bleeding fissures (Fig. 1c). Although she had therapy with oral retinoids and local application of white petrolatum, in a humid incubator, her clinical symptoms failed to show any apparent improvement and she died when she was 5 months old.

Skin biopsies showed thick stratum corneum in both patients (Fig. 1d–g). In Patient 2, parakeratosis was observed in the epidermis and a sparse inflammatory cell infiltration was seen in the superficial dermis (Fig. 1e inset). Electron microscopy (Hitachi, Tokyo, Japan) revealed a large number of abnormal, variously sized lipid droplets that accumulated in the cornified cells of both patients' epidermis.

Mutational analysis of *ABCA12* was performed in both patients and their families. Each genomic DNA sample was subjected to PCR amplification, followed by direct automated sequencing. Oligonucleotide primers and PCR conditions used for amplification of all exons 1–53 of *ABCA12* were originally derived from the report by Lefèvre et al. [5] and were partially modified for the present study. The entire coding region including the exon/intron boundaries for both forward and reverse strands from the patients, their parents and 50 healthy Japanese controls were also sequenced. Both patients had the same paternal novel nonsense mutation p.Arg1515X (Fig. 1h) which leads to truncation of the first ATP-binding cassette within ABCA12 likely resulting in ABCA12 loss of function (Fig. 2a). On the other allele, Patient 1 had a maternal recurrent splice acceptor site mutation c.3295-2A>G (Fig. 1h). This splice site mutation was reported in an unrelated Japanese family with HI and was shown to lead to comparable amounts of 2 splice pattern variants [2]. The first mutant transcript would result in a 3 amino acids deletion (1099_1101delYMK). These 3 amino acids are located in the first transmembrane domain and are highly conserved (Fig. 2b). The second mutant transcript lost a 170-bp sequence from exon 24, which led to a frameshift. Expression of a small amount of ABCA12 protein, although mutated, was detected in the granular layer keratinocytes of the patient's epidermis and cultured keratinocytes by immunofluorescent staining [2]. Thus, it is possible that Patient 1 expresses some mutated ABCA12 protein with a partial function. This might be the reason why Patient 1 survived beyond the perinatal and neonatal period and is still alive although this might also be in part due to the prompt oral retinoid treatment.

Patient 2 carried a maternal missense mutation p.Gly1179Arg on the other locus (Fig. 1h). To confirm the presence of the mutation p.Gly1179Arg in Patient 2, we performed restriction enzyme digestion analysis using *BclI* (NEW ENGLAND BioLabs). Restriction enzyme digestion of PCR products was carried out according to the manufacture's protocols. The 255-bp PCR products from wild type alleles were not digested by *BclI*, although the PCR products from the allele with the mutation p.Gly1179Arg were digested into 173- and 82-bp fragments. The father's PCR product after *BclI* digestion showed a single 255-bp band, which indicated he had only normal alleles. In contrast, the PCR product after *BclI* digestion from the mother of Patient 2 showed 255-, 173- and 82-bp bands, which indicated that she was heterozygous for the p.Gly1179Arg missense mutation (supplementary Fig. S1). This mutation was reported in a

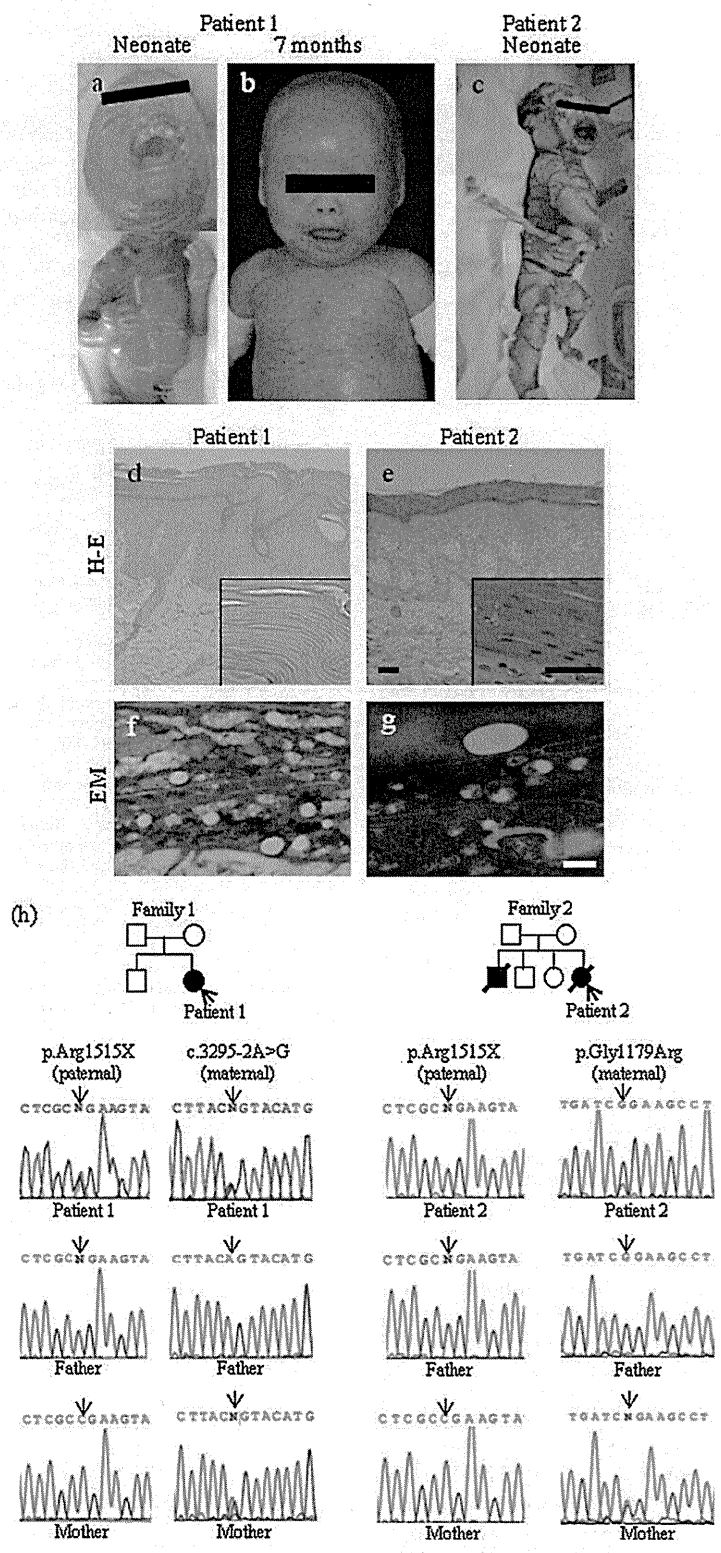

Fig. 1. (a–c) Clinical features of HI patients. Patient 1 showed the typical clinical phenotype of HI during the neonatal period, including the face and trunk (a). Her clinical symptoms remarkably improved at 7 months of age (b). Patient 2 showed more serious symptoms with thick plate-like scales and skin fissures in the neonatal period (c) and lived until the age of 5 months. (d–g) Histological features of the skin lesions of HI patients. Skin biopsies showed thick stratum corneum in both patients. Bars, 50 μm (d and e). In Patient 2, parakeratosis were observed (e, inset). By electron microscopy, abnormal variously sized lipid droplets had accumulated in the cornified cells of both patients' epidermis. Bars, 200 nm (f and g). (h) Families with HI and *ABCA12* mutations. Patient 1 was a compound heterozygote for two *ABCA12* mutations, a novel nonsense mutation p.Arg1515X and a recurrent splice site mutation c.3295-2A>G, and both her parents were heterozygous carriers. Patient 2 harboured two *ABCA12* mutations, p.Arg1515X and p.Gly1179Arg, and both her parents were heterozygous carriers of these defects.

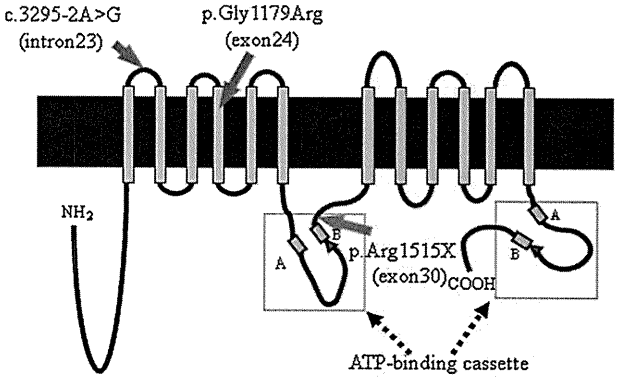

c.3295-2A>G: 1099_1101delYMK

Homo sapiens	1089	VYEKDLRLHEYMKMMGVNSCSHF 1111
Rattus norvegius		VYEKDLRLHEYMKMMGVNSCSHF
Mus musculus		VYEKDLRLHEYMKMMGVNSCSHF
Gallus gallus		VQEKDLRLYEYMKMMGVNASSHF
Danio rerio		VHERELRLHEYMKMMGVNPISHF

p.Gly1179Arg

Homo sapiens	1165	ISVFFNNTNIAALIGSLIYIIAFFPFIVL 1193
Rattus norvegius		ISVFFNNTNIAALIGSLIYVIAFFPFIVL
Mus musculus		ISVFFNNTNIAALIGSLIYVIAFFPFIVL
Gallus gallus		ISVFFNNTNIAALVGSLVYILTFFPFIVL
Danio rerio		VSSFFDKTNIAGLSGSLIYVISFFPFIVL

Fig. 2. (a) Structure of ABCA12 protein and the three mutations in present HI families. Dark blue area, cell membrane; bottom of dark-blue area, cytoplasmic surface. Note the mutation shared between the two patients is a truncation mutation in the first ATP-binding cassette (p.Arg1515X). The other mutation in Patient 2 is just a missense mutation in the first cluster of transmembrane domains (p.Gly1179Arg). (b) ABCA12 amino acid sequence alignment shows the level of conservation in diverse species of the amino acids, 1099_1101delYMK and p.Gly1179Arg (red characters).

Laotian family [6]. The glycine 1179 is a highly conserved amino acid residue (Fig. 2b) located in the first transmembrane ABCA12 domain (Fig. 2a), and this mutation substitutes an uncharged polar glycine residue for a positively charged arginine residue. The presence of these mutations was excluded in 100 alleles of 50 normal unrelated Japanese individuals.

Determinants of genotype/phenotype correlations resulting from *ABCA12* mutations, typically demonstrate that homozygotes or compound heterozygotes with truncation *ABCA12* mutations lead to an HI phenotype. Only a few exceptional cases have been reported such as the present case. The mutation p.Gly1179Arg might result in major loss of ABCA12 function and/or structure, leading to the severe phenotype in Patient 2.

Recently, long-term survival of patients with HI has been more frequently observed and documented [7,8]. The clinical symptoms of Patient 1 showed a remarkable improvement during infancy. In contrast, the symptoms of Patient 2 did not improve, and she died at the age of 5 months. The marked difference in the clinical severity of the two patients indicated that the p.Gly1179Arg has far bigger deleterious functional effects than c.3295-2A>G. The present study clearly demonstrates that some missense *ABCA12* mutations within highly conserved transmembrane regions are able to cause drastic changes in protein structure and function, leading to severe phenotypes, similar to truncation mutation patients. Further accumulation of similar cases is needed to confirm genotype/phenotype correlation in *ABCA12* mutations, especially in studies involving missense mutations underlying HI.

Acknowledgments

We thank Dr. James R. McMillan for proofreading the manuscript. This work was supported in part by a grant-in-aid from the Ministry of Education, Science, Sports and Culture of Japan (Kiban B 20390304: to M.A.), a grant from Ministry of Health, Labour and Welfare of Japan (Health and Labour Sciences Research Grants; Research on Intractable Disease: H22-177: to M.A.).

Appendix A. Supplementary data

Supplementary data associated with this article can be found, in the online version, at doi:10.1016/j.jdermsci.2010.11.010.

References

[1] Akiyama M. Harlequin ichthyosis and other autosomal recessive congenital ichthyoses: the underlying genetic defects and pathomechanisms. J Dermatol Sci 2006;42:83–9.
[2] Akiyama M, Sugiyama-Nakagiri Y, Sakai K, McMillan JR, Goto M, Arita K, et al. Mutations in ABCA12 in harlequin ichthyosis and functional rescue by corrective gene transfer. J Clin Invest 2005;115:1777–84.
[3] Kelsell DP, Norgett EE, Unsworth H, Teh MT, Cullup T, Mein CA, et al. Mutations in ABCA12 underlie the severe congenital skin disease harlequin ichthyosis. Am J Hum Genet 2005;76:794–803.
[4] Akiyama M. ABCA12 mutations and autosomal recessive congenital ichthyosis: a review of genotype/phenotype correlations and of pathogenetic concepts. Hum Mutat 2010;31(July):1090–6.
[5] Lefèvre C, Audebert S, Jobard F, Bouadjar B, Lakhdar H, Boughdene-Stambouli O, et al. Mutations in the transporter ABCA12 are associated with lamellar ichthyosis type 2. Hum Mol Genet 2003;12:2369–78.
[6] Thomes AC, Cullup T, Norgett EE, Hill T, Barton S, Dale BA, et al. ABCA12 is the major harlequin ichthyosis gene. J Invest Dermatol 2006;126:2408–13.
[7] Akiyama M, Sakai K, Sato T, McMillan JR, Goto M, Sawamura D, et al. Compound heterozygous ABCA12 mutations including a novel nonsense mutation underlie harlequin ichthyosis. Dermatology 2007;215:155–9.
[8] Akiyama M, Sakai K, Wolff G, Hausser I, McMillan JR, Sawamura D, et al. A novel ABCA12 mutation 327delT causes harlequin ichthyosis. Br J Dermatol 2006;155:1064–6.

H. Umemoto[a,b]
[a]*Department of Dermatology, Hokkaido University Graduate School of Medicine, Sapporo, Japan*
[b]*Department of Oral Diagnosis and Oral Medicine, Hokkaido University Graduate School of Dental Medicine, Sapporo, Japan*

M. Akiyama[a,b,*]
[a]*Department of Dermatology, Hokkaido University Graduate School of Medicine, Sapporo, Japan*
[b]*Department of Dermatology, Nagoya University Graduate School of Medicine, Nagoya, Japan*

T. Yanagi
K. Sakai
Department of Dermatology, Hokkaido University Graduate School of Medicine, Sapporo, Japan

Y. Aoyama
Department of Dermatology, Okayama University Graduate School of Medicine, Okayama, Japan

A. Oizumi
Y. Suga
Department of Dermatology, Juntendo University School of Medicine, Urayasu Hospital, Urayasu, Japan

Cell Stem Cell
Article

Hair Follicle Stem Cells Provide a Functional Niche for Melanocyte Stem Cells

Shintaro Tanimura,[1,2,9] Yuko Tadokoro,[1,9] Ken Inomata,[1,3] Nguyen Thanh Binh,[1,8] Wataru Nishie,[2] Satoshi Yamazaki,[4,5] Hiromitsu Nakauchi,[4,5] Yoshio Tanaka,[1] James R. McMillan,[2] Daisuke Sawamura,[6] Kim Yancey,[7] Hiroshi Shimizu,[2] and Emi K. Nishimura[1,2,8,*]

[1]Department of Stem Cell Medicine, Cancer Research Institute, Kanazawa University, Kanazawa, Ishikawa 920-0934, Japan
[2]Department of Dermatology, Hokkaido University Graduate School of Medicine, Sapporo 060-8638, Japan
[3]Fundamental Research Laboratories, KOSÉ Corporation, 1-18-4 Azusawa, Itabashi-ku, Tokyo 174-0051, Japan
[4]Japan Science and Technology Agency (JST), ERATO, Sanbacho, Chiyoda-ku, Tokyo 102-0075, Japan
[5]Division of Stem Cell Therapy, Center for Stem Cell Biology and Regenerative Medicine, The Institute of Medical Science, The University of Tokyo, 4-6-1 Shirokanedai, Minato-ku, Tokyo 108-8639, Japan
[6]Department of Dermatology, Hirosaki University, School of Medicine, Hirosaki, Aomori 036-8562, Japan
[7]Department of Dermatology, University of Texas Southwestern Medical Center in Dallas, Dallas, TX 75390-9069, USA
[8]Department of Stem Cell Biology, Medical Research Institute, Tokyo Medical and Dental University, 2-3-10 Kanda Surugadai, Chiyoda-ku, Tokyo 101-0062, Japan
[9]These authors contributed equally to this work
*Correspondence: nishscm@tmd.ac.jp
DOI 10.1016/j.stem.2010.11.029

SUMMARY

In most stem cell systems, the organization of the stem cell niche and the anchoring matrix required for stem cell maintenance are largely unknown. We report here that collagen XVII (COL17A1/BP180/BPAG2), a hemidesmosomal transmembrane collagen, is highly expressed in hair follicle stem cells (HFSCs) and is required for the maintenance not only of HFSCs but also of melanocyte stem cells (MSCs), which do not express *Col17a1* but directly adhere to HFSCs. Mice lacking *Col17a1* show premature hair graying and hair loss. Analysis of *Col17a1*-null mice revealed that COL17A1 is critical for the self-renewal of HFSCs through maintaining their quiescence and immaturity, potentially explaining the mechanism underlying hair loss in human *COL17A1* deficiency. Moreover, forced expression of *COL17A1* in basal keratinocytes, including HFSCs, in *Col17a1*-null mice rescues MSCs from premature differentiation and restores TGF-β signaling, demonstrating that HFSCs function as a critical regulatory component of the MSC niche.

INTRODUCTION

The stem cell microenvironment, or niche, is critical for stem cell maintenance (Li and Xie, 2005; Moore and Lemischka, 2006). Accumulating evidence has confirmed that cell-cell and cell-extracellular matrix adhesion within the niche is essential for the establishment and maintenance of niche architecture in different stem cell systems (Raymond et al., 2009). Adhesion to the underlying extracellular matrix has been suggested as an important factor in epidermal stem cell maintenance (Green, 1977; Watt, 2002), but a specific stem-cell anchoring matrix for stem cell maintenance has not yet been identified. Hair follicle stem cells (HFSCs) are found in the hair follicle bulge, a distinct area of the outer root sheath that overlies the basement membrane at the lower permanent portion in mammalian hair follicles (Blanpain and Fuchs, 2006; Cotsarelis, 2006). The HFSC population is composed of multipotent keratinocyte stem cells and is responsible for the cyclic regeneration of hair follicles as well as a transient supply of progeny to the interfollicular epidermis (IFE) and to sebaceous glands after wounding (Blanpain and Fuchs, 2006; Cotsarelis, 2006; Oshima et al., 2001). The HFSC population in the bulge area normally supplies a short-term reservoir to the secondary hair germ (subbulge area), which is located just below the bulge area but above the dermal papilla and corresponds to the lowermost portion of resting hair follicles (Figure S1A available online; Greco et al., 2009). Melanocyte stem cells (MSCs), which are originally derived from the neural crest, also reside in the follicular bulge-subbulge area (Figure S1A). MSCs supply pigment-producing melanocytes to the hair matrix during each hair cycle to maintain hair pigmentation (Nishimura et al., 2002). Therefore, the bulge-subbulge area houses at least two distinct stem cell populations with different origins. However, it is still unclear to what extent these two different stem cells interact to promote each other's maintenance.

Hemidesmosomes are multiprotein adhesion complexes that promote stable epidermal-dermal attachments. The transmembrane protein collagen XVII (COL17A1/BP180/BPAG2) is a structural component of the outer hemidesmosomal plaque, which projects beneath hemidesmosomes in epidermal basal keratinocytes into the underlying basement membrane to mediate anchorage (Masunaga et al., 1997; Nishizawa et al., 1993; Powell et al., 2005). In patients with *COL17A1* deficiency, a subtype of congenital junctional epidermolysis bullosa blistering disease, hemidesmosomes are poorly formed (McGrath et al., 1995; Nishie et al., 2007) and there is a characteristic premature hair loss (alopecia) with hair follicle atrophy (Darling et al.,

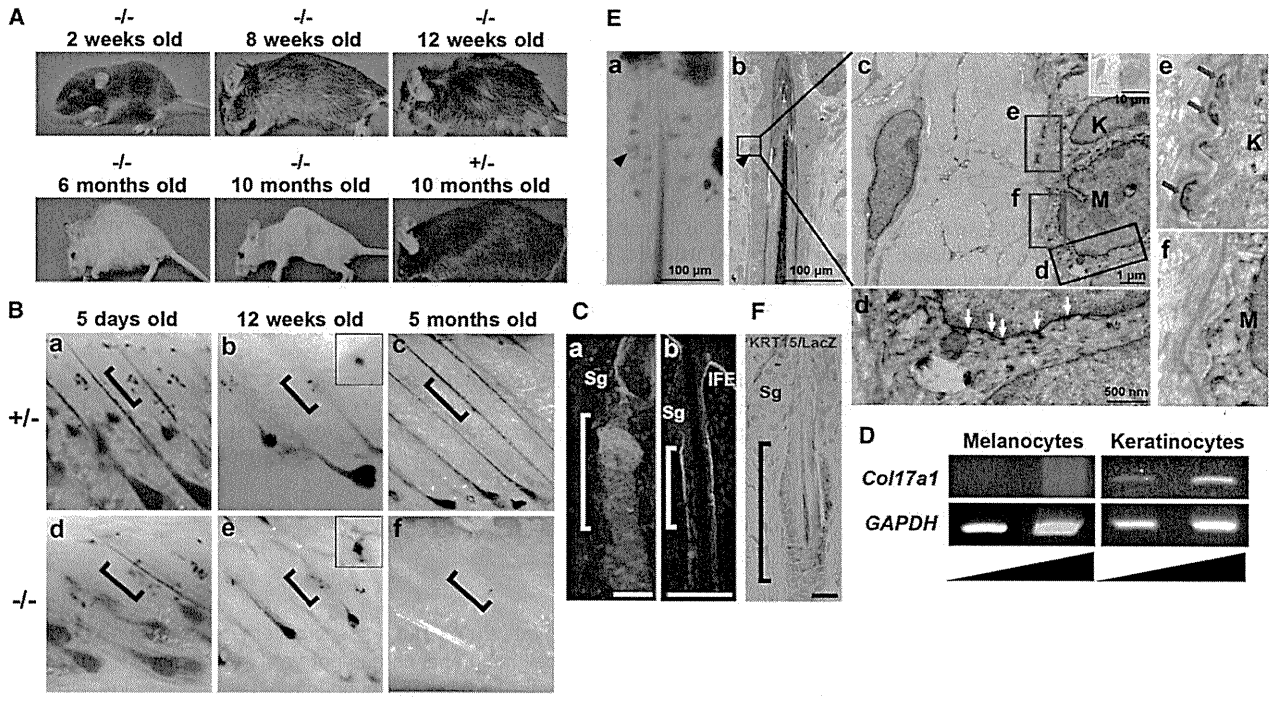

Figure 1. Hair Graying and Hair Loss Are Preceded by Depletion of MSCs in *Col17a1* Deficiency

(A) Macroscopic phenotype of *Col17a1*$^{-/-}$ mice at different times as noted and of *Col17a1*$^{+/-}$ littermates at 10 months of age.

(B) Deletion of *Col17a1* affects the maintenance of MSCs in the bulge-sububulge area. The distribution and morphology of *Dct-lacZ*-expressing melanoblasts is normal in the bulge-subbulge area of 5-day-old *Col17a1*$^{-/-}$ mice (a and d). At 12 weeks of age, abnormal melanocytes with dendritic morphology were found in the bulge area of *Col17a1*$^{-/-}$ anagen follicles (e). Inset in (e) shows magnified view of ectopically pigmented melanocytes in the hair follicle bulge-subbulge of *Col17a1*$^{-/-}$ mice. By 5 months of age, *Dct-lacZ*-expressing cells were lost both in the bulge-subbulge area and in the hair bulb (f). Bulge-subbulge areas are demarcated by brackets.

(C) COL17A1 expression in the bulge area (demarcated by brackets). (a) COL17A1 (a: red) is expressed in KRT15 (a: green)-expressing bulge keratinocytes and in basal cells of the IFE (b: green) in wild-type skin. (b) *Dct-lacZ*-expressing melanoblasts (b: red) are located close to COL17A1^{+} basal cells (b: green) in wild-type follicles. Scale bars represent 40 μm.

(D) RT-PCR analysis; the level of *Col17a1* mRNA is below the detection limit in flow cytometry-sorted GFP-tagged melanoblasts.

(E) Light and electron micrographs of *Dct-lacZ*-expressing melanoblasts in the bulge area (MSCs). The arrowheads in (a) and (b) point to *Dct-lacZ*-expressing melanocytes in the bulge areas in semithin sections of the skin. The ultrastructural high-power view is of the boxed areas shown in (b) and (c). X-gal reaction products accumulated in association with the nuclear membrane (d: white arrows). *Dct-lacZ*-expressing melanocytes lack hemidesmosome formation in the basement membrane zone (f), whereas adjacent keratinocytes form mature hemidesmosomes in the bulge area (e: red arrows).

(F) *Dct-lacZ*-expressing melanoblasts (blue) are in direct contact with keratin 15 (KRT15)-expressing keratinocytes in the bulge area (yellow brown). Scale bar represents 20 μm.

M, melanocytes in bulge; K, keratinocytes in bulge; Sg, sebaceous gland; IFE, interfollicular epidermis. See also Figure S1.

1997; Hintner and Wolff, 1982) that suggests that COL17A1 plays a role in hair follicle homeostasis. We previously reported premature hair loss in *Col17a1*-deficient mice (Nishie et al., 2007), although the precise underlying mechanism is unknown. In this study, we used *Col17a1* knockout mice and *COL17A1*-expressing transgenic mice to show that *Col17a1* plays essential roles in the maintenance of HFSCs, which provide a functional niche for MSCs.

RESULTS

Defective MSC Maintenance and Resultant Hair Graying in *Col17a1*-Null Mice

To understand the role of collagen XVII in hair follicle homeostasis, we performed a careful chronological analysis of *Col17a1*-deficient mice. As shown in Figure 1A, *Col17a1* null mice showed premature hair loss generally preceded by extensive hair graying. Conversely, heterozygous mice displayed a normal phenotype. The hair coats in *Col17a1*-null mice were indistinguishable from control littermates for 8 weeks after birth. However, progressive hair graying started from the snout at around 12 weeks of age and then became pronounced on their backs at around 4–6 months of age and was associated with a sparser hair distribution that was subsequently followed by progressive and more extensive hair loss (Figure 1A). It is notable that these hair changes were not accompanied or preceded by any apparent changes in the skin. Skin friction, such as attempting to artificially peel neonatal skin, can induce skin erosions in *Col17a1*-null mice (Nishie et al., 2007) but did not significantly accelerate hair graying or hair loss. Thus, it is unlikely that the hair changes are a secondary outcome of skin detachment but is more likely that the hair graying and hair loss are programmed through the

Col17a1 deficiency in the hair follicles. Our previous studies demonstrated that defective maintenance of MSCs in the hair bulge causes hair graying (Nishimura et al., 2005). Thus, we first examined the distribution and morphology of MSCs in *Col17a1*-null mice by using a melanocyte-targeted *Dct-lacZ* transgene (Mackenzie et al., 1997). As shown in Figures 1Ba and 1Bd, *Dct-lacZ*-expressing cells showed a normal morphology and distribution in the bulge area during hair follicle morphogenesis until initiation of the hair regeneration cycle both in *Col17a1*$^{+/-}$ and in *Col17a1*$^{-/-}$ mice. At around 12 weeks after birth, pigmented melanocytes with a dendritic morphology that expressed melanocyte markers appeared in the hair follicle bulge of *Col17a1*$^{-/-}$ mice (Figure 1Be; Figure S1Be). At 5 months of age, *Dct-lacZ*-expressing cells were almost completely lost in the follicle bulge area as well as in the hair bulbs of *Col17a1*-null mice (Figure 1Bf; Figure S1Bf). These data demonstrate that MSC maintenance is defective in *Col17a1*-deficient mice and that this mechanism results in progressive hair graying.

Preferential Expression of COL17A1 in HFSCs but Not in MSCs

Collagen XVII is a hemidesmosomal transmembrane collagen expressed by basal keratinocytes of the IFE (McGrath et al., 1995). However, neither the expression of mouse *Col17a1* nor hemidesmosome assembly in melanocyte lineage cells and/or in bulge keratinocytes has been reported, so we first examined the expression of mouse COL17A1 protein in hair follicles by using immunohistochemistry. As shown in Figure 1Ca and Figures S1C and S1D, mouse COL17A1 was preferentially localized along the dermal-epidermal junction of bulge keratinocytes that express markers for HFSCs but not in follicular keratinocytes outside of the bulge area. However, the localization of COL17A1 in basal cell surface of MSCs could not be determined via normal immunohistochemical methods, because the attachment site of MSCs to the basement membrane is limited (Figure 1Cb). We therefore examined *Col17a1* expression by using RT-PCR in flow cytometry-sorted GFP^{+} cells from melanocyte lineage-tagged GFP transgenic mouse skin (Osawa et al., 2005). In sharp contrast to the significant expression of *Col17a1* in control keratinocytes, expression in GFP^{+} melanocytes was not detectable (Figure 1D). To support this finding, we used transmission electron microscopy (TEM) to check whether *Dct-lacZ*-expressing melanoblasts within the bulge area in wild-type animals have hemidesmosomes. As shown in Figure 1E, hemidesmosomes, which form regularly spaced electron-dense structures along the epidermal basement membrane zone (McMillan et al., 2003), were completely absent in *Dct-lacZ*-expressing melanoblasts in the bulge (Figures 1Ed and 1Ef), whereas typical hemidesmosomes were seen overlying the basal plasma membrane in surrounding bulge keratinocytes (Figure 1Ee). Because these bulge keratinocytes adjacent to *Dct-lacZ*-expressing melanoblasts express HFSC markers (Figure 1F), these data indicate that HFSCs but not MSCs are anchored to the underlying basement membrane via hemidesmosomes. We also confirmed the localization of COL17A1 to hemidesmosomes in basal keratinocytes but not in melanocytes by immunogold electron microscopic analysis of human epidermis (Figure S1E). Therefore, we conclude that MSCs do not express COL17A1 and do not assemble any discernible hemidesmosomal structures at their surface. These findings suggested that the depletion of MSCs in *Col17a1*-null mice is caused by defects in the HFSC population that forms the main supportive cells surrounding MSCs.

Abrogated Quiescence and Immaturity of HFSCs Result in Depletion of HFSCs in *Col17a1*-Null Mice

Previous studies on wild-type mouse skin reported that mature hemidesmosomes exist at the follicular-dermal junction just below the level of sebaceous glands (Hojiro, 1972) and in hair germs of telogen hair follicles (Greco et al., 2009). Consistently, we found mature hemidesmosomes at these junctions within the hair follicle bulge (Figure 1Ee). However, mature hemidesmosomes have not been found in the transient portion of hair follicles (Hojiro, 1972), where COL17A1 expression is undetectable. These data suggested that hemidesmosome formation is important for anchoring of HFSCs located in the bulge-subbulge area of hair follicles to the basal lamina.

To test whether the abnormalities observed in *Col17a1* deficiency are specifically caused by any functional defects of HFSCs or by their detachment from the basal lamina, we first carefully examined the junctions of hair follicles in the dorsal skin of *Col17a1*-null mice and their controls by TEM. A significant number of hemidesmosomes are poorly formed in the bulge keratinocytes of *Col17a1*-deficient mice (Figure S2B), as seen in epidermal keratinocytes of those mice (Nishie et al., 2007). However, we did not find any significant microscopic separation at the follicular-dermal junction in sections of trunk skin from *Col17a1*-null mice (Figure 2; Figures S2A and S2B). Furthermore, we did not find significant inflammatory cell infiltrates or any signs of cell death, such as the appearance of eosinophilic cell bodies or TUNEL-positive or cleaved caspase 3-positive cells, at the follicular-dermal junction area of *Col17a1*-null mouse skin (Figure S2C and data not shown). Basement membrane thickening/reduplication, a sign of repeated regeneration of the epidermal and dermal junction, was also not found. These findings suggested that the hair graying and hair loss phenotypes in *Col17a1*-null mice cannot be explained simply by HFSC detachment from the basal lamina but instead may result from dysregulation or altered cell properties of HFSCs caused by *Col17a1* deficiency.

To examine whether HFSCs show any dysregulation caused by *Col17a1* deficiency, we carefully examined the hair follicle cycle progression, which alternates phases of growth (anagen), regression (catagen), and rest (telogen) in synchronization with the activation status of HFSCs, in *Col17a1*-null mice. While the first short telogen phase was transiently seen around 22 days after birth both in *Col17a1*-null mice and in control littermates, the second telogen phase was significantly shortened in *Col17a1*-null mice (Figure 2, summarized on the right side). At 6 weeks of age, just before normal hair follicles on the dorsal skin enter the second telogen phase, most hair follicles in *Col17a1*$^{-/-}$ mice were not distinguishable from those in *Col17a1*$^{+/-}$ mice either in morphology or in hair cycle progression. The second telogen phase is normally seen at around 7 weeks after birth and lasts about 4–5 weeks over the entire skin surface of wild-type mice (Paus and Cotsarelis, 1999; Paus et al., 1999). This phase was shortened to less than 2 weeks in all *Col17a1*$^{-/-}$ mice examined at 8–12 weeks of age, whereas such an aberrant pattern was seen in only 14.3% of *Col17a1*$^{+/-}$ mice. The subsequent

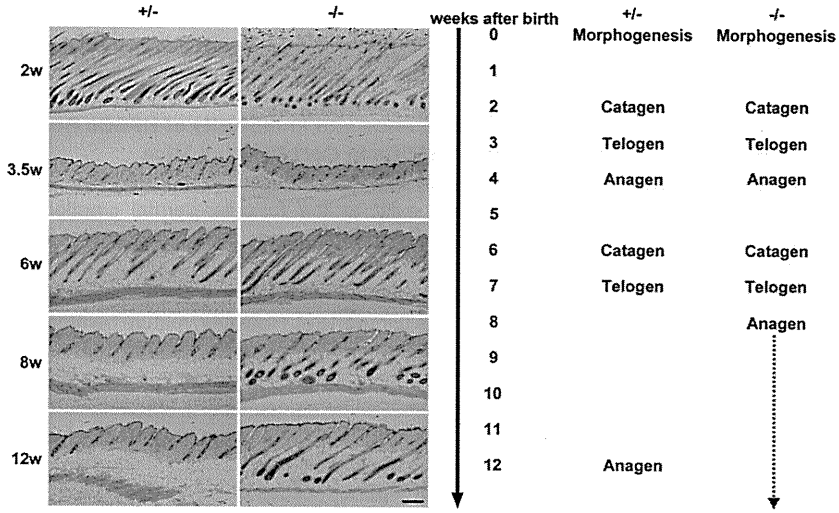

Figure 2. Loss or Shortening of the Resting State of Hair Follicles in *Col17a1*-Deficient Skin

Representative H&E images of dorsal skin sections (left) and time-scale for the hair cycle (right) from *Col17a1*$^{-/-}$ mice and from *Col17a1*$^{+/-}$ littermates during the first 12 weeks after birth. In *Col17a1*$^{-/-}$ follicles, the second telogen was significantly shortened, and the second anagen lasted longer. Scale bar represents 200 μm. See also Figure S2.

anagen phase was rather prolonged in *Col17a1*$^{-/-}$ mice compared to their control littermates. These findings suggest that HFSCs are unable to remain quiescent for a sufficient time from the second telogen phase and thereafter in the absence of *Col17a1*.

To search for early events or changes in HFSCs in *Col17a1*-null mice, we performed immunohistochemical analysis with four different markers for HFSCs, keratin 15 (KRT15), CD34, α6-integrin, and S100A6, at different stages (Figure 3A; Figure S3; Morris et al., 2004; Tumbar et al., 2004). At 5 weeks of age, there was no difference in the expression of HFSC markers or the number of HFSC marker-positive cells between control and *Col17a1*-null mice. However, at around 8 weeks of age, HFSC marker-expressing cells were absent in the bulge area in selected null mouse hair follicles (Figures 3A and 3B; Figure S3A), and the number of these marker-deficient follicles increased over time. By 6 months of age, the HFSC population had been lost in most hair follicles of *Col17a1*-null mice (Figure S3B). Flow cytometric analysis also confirmed that the α6-integrin^{high} CD34^{+} population (Blanpain and Fuchs, 2006), which represents basal HFSCs in the bulge area, was diminished (Figure 3C). Hair follicle atrophy with the loss of hair follicle structures were also observed once the HFSC population was diminished (Figure 3D). These data indicate that *Col17a1*-null HFSCs fail to maintain their stem cell characteristics, including their quiescence and immaturity, after the second telogen phase, resulting in hair follicle atrophy. Conversely, epidermal hyperplasia was also transiently found in some focal areas of the *Col17a1*-null skin at around 6 months of age (Figure 3D, arrowheads) but was normalized and subsequently became atrophic at later stages, which suggests that the epidermal stem cell population might also be gradually losing its self-renewing potential with age in *Col17a1* deficiency compared to controls.

To examine whether HFSC maintenance fails because the cells lose their immaturity or quiescence in the absence of *Col17a1*, we analyzed the expression of markers for keratinocyte differentiation and proliferation in *Col17a1*-null hair follicles. Interestingly, keratin 1 (KRT1), a differentiation marker for the IFE, was ectopically expressed in the bulge area of *Col17a1*-null mice at 8 weeks of age (Figure 4A). KRT1-positive cells in the bulge areas of affected hair follicles were found in 60% of *Col17a1*-null mice but not in control mice at that age. Ectopic expression of other epidermal differentiation markers, such as involucrin and KRT10, was also present in the bulge areas of *Col17a1*-null mice at 8 weeks of age (Figure S4A). Furthermore, Ki67-positive cells were located in the bulge area of *Col17a1*-null mice, and those Ki67-positive cells showed an absent or reduced level of KRT15 expression (Figure 4A).

The maintenance of quiescence and immaturity of somatic stem cells in tissues is a prerequisite for sustained stem cell self-renewal, and which can be assessed for HFSCs by means of a colony-formation assay in vitro (Barrandon and Green, 1987; Oshima et al., 2001). We therefore took advantage of the type of assay by using neonatal epidermal keratinocytes, which contain the presumptive HFSC population (Nowak et al., 2008), to assess the self-renewal potential of that population in *Col17a1*-null mice. As shown in Figures 4Ba and 4Bb, *Col17a1* homozygous null keratinocytes showed defects in colony-forming ability on 3T3-J2 feeder cells compared to keratinocytes from control mice. Colonies larger than 0.5 mm in diameter were significantly decreased in number with *Col17a1*-null keratinocytes (Figure 4Bc). Although *Col17a1*-null keratinocytes showed defective binding ability to collagen I-coated dishes (Figure S4B), they showed no detectable defects in their ability to directly adhere to 3T3-J2 feeder cells (Figure 4Bd). These data strongly suggest that *Col17a1*-null keratinocytes have a much lower renewal capability than control keratinocytes. Taken together with the in vivo findings, we conclude that COL17A1 is critical for the self-renewal of HFSCs by maintaining their immaturity and quiescence.

Loss of TGF-β Expression by HFSCs and the Associated Differentiation of Adjacent MSCs

To examine whether the early changes in HFSC in *Col17a1* mutant mice affects the maintenance of MSCs in the hair follicle bulge, we carefully examined MSCs in hair follicle bulge areas in *Col17a1*-null mice beginning to show HFSC defects. At 8 weeks of age, when HFSCs in *Col17a1*-null mice are prematurely activated, KIT^{+} melanoblasts within the bulge area prematurely coexpressed TYRP1, a melanocyte differentiation marker, in *Col17a1*-null mice but not in control mice (Figure S5A). At around 12 weeks of age, pigmented melanocytes with a mature

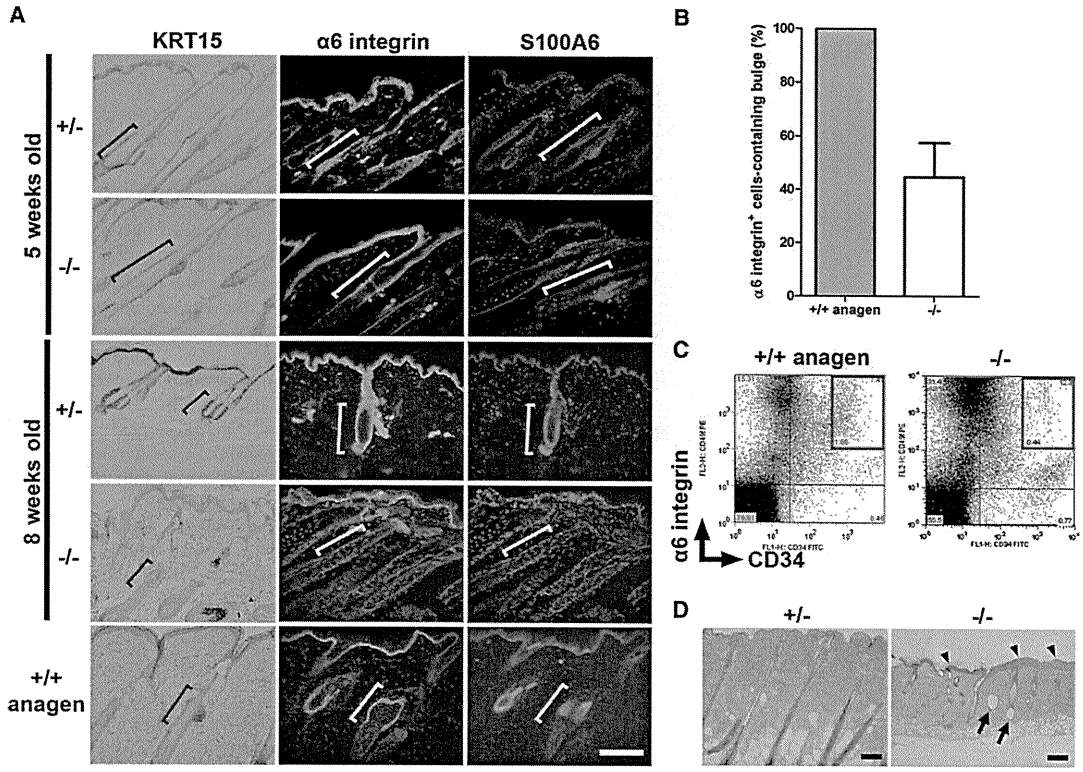

Figure 3. HFSC Depletion in COL17A1-Deficient Mice

(A) Immunostaining of the dorsal skin from *Col17a1*$^{-/-}$ and from *Col17a1*$^{+/-}$ mice with HFSC markers. The bulge areas are demarcated by brackets. HFSC marker (KRT15, α6-integrin, and S100A6)-expressing cells were still maintained at 5 weeks of age in *Col17a1*$^{-/-}$ mice, whereas follicles without HFSC marker-positive cells appeared at 8 weeks of age.

(B) Ratio of hair follicles with α6-integrin^{+} cells in the bulge areas of skin from control mice and from 8- to 10-week-old *Col17a1*$^{-/-}$ mice. In *Col17a1*$^{-/-}$ mice, many hair follicles without α6-integrin^{+} cells in the bulge areas were found (n = 3).

(C) Flow cytometric analysis of α6-integrin and CD34 double-labeled keratinocytes. α6-integrin^{+} CD34^{+} cells are almost completely lost in the skin of 9-month-old *Col17a1*$^{-/-}$ mice.

(D) H&E-stained histological sections of *Col17a1*$^{-/-}$ and of *Col17a1*$^{+/-}$ mouse skin. At 6 months of age, there was a diminution of hair follicle bulbs, degeneration of the hair follicles (arrows), and epidermal hyperplasia (arrowheads) in *Col17a1*$^{-/-}$ skin. As a control for the anagen phase in (A), (B), and (C), dorsal skin at 5 days after hair-plucking of telogen follicles was used.

Scale bars represent 100 μm. See also Figure S3.

dendritic morphology and expressing TYRP1 in addition to *Dct-lacZ* and KIT were aberrantly found within the bulge area in mid-anagen hair follicles (*Dct-lacZ*-expressing cells in Figure 1B, Figure S1B, arrow in Figure 5A; KIT^{+}/TYRP1^{+} cells in Figures 5B and 5C and Figure S5B). Conversely, only nonpigmented melanoblasts expressing *Dct-lacZ* and KIT but not TYRP1 and with small cell bodies (MSCs) were found in control littermates (Figure 1B; Figures S1B and S5B). Similar morphological changes were previously described as ectopic MSC differentiation within the niche (Inomata et al., 2009; Nishimura et al., 2005). These ectopically differentiated melanocytes were found in the bulge area at 12–13 weeks of age, prior to the hair graying seen in *Col17a1*-null mice (Figure 5D). Furthermore, it is notable that the ectopically differentiated melanocytes in *Col17a1*-deficient mice were typically found in association with early changes in bulge keratinocytes including the enlarged morphology of surrounding bulge keratinocytes (Figure 5A, arrowheads) and an increased number of Ki67-expressing bulge keratinocytes in midanagen follicles (Figures 4A and 5E and data not shown). The appearance of ectopically differentiated melanocytes within the bulge area was followed by progressive hair graying in *Col17a1*-null mice (Figures 1A and 1B; Figure S1B).

TGF-β signaling is activated in the hair follicle bulge and is involved in but is not essential for the maintenance of HFSCs (Guasch et al., 2007; Qiao et al., 2006; Yang et al., 2005, 2009). Our recent study showed that the signal is required for the maintenance of MSCs through promoting MSC immaturity and quiescence (Nishimura et al., 2010), but it was not clear whether the signal is derived from HFSCs or MSCs. As similar changes in MSCs, such as the appearance of ectopically differentiated melanocytes in the niche and the subsequent depletion of MSCs seen in *Col17a1*-null mice, were found in *TGFbRII* conditional knockout mice (Nishimura et al., 2010), we hypothesized that the defective renewal of MSCs in *Col17a1*-null mice might be mediated by defective TGF-β signaling from the surrounding HFSCs. To test this model, we examined the involvement of TGF-β signaling in the defects of MSCs in *Col17a1*-null mice and their controls. We found that KRT15-expressing

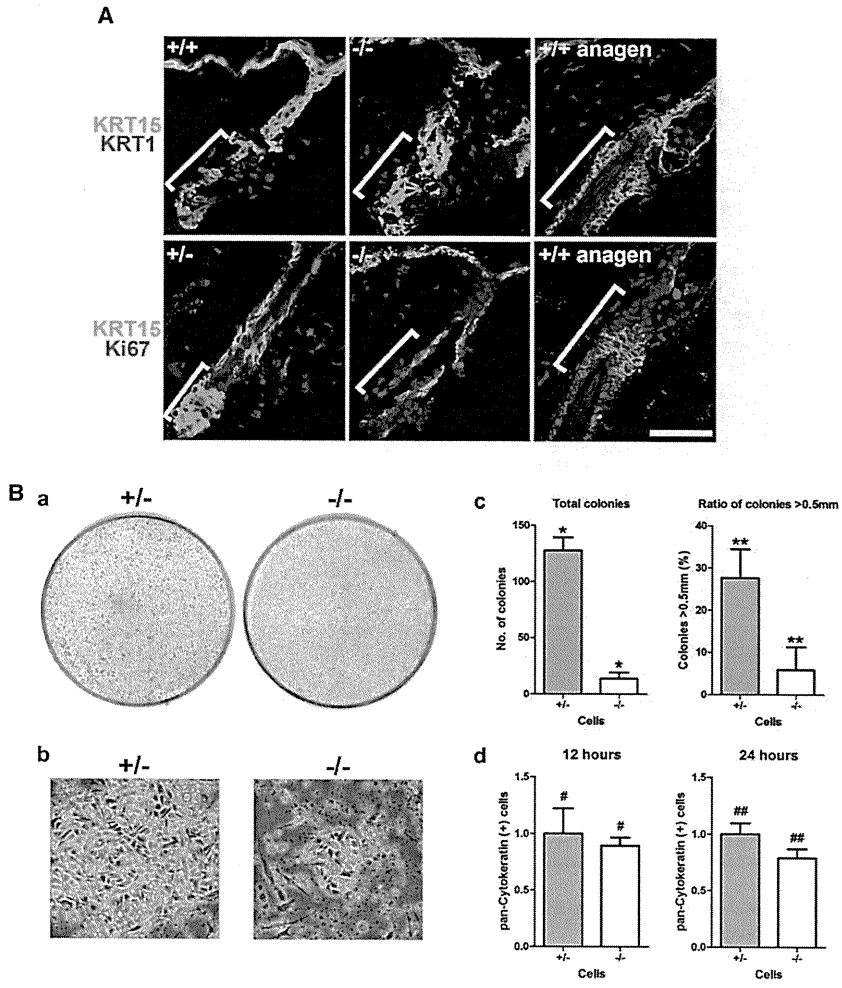

Figure 4. Deficient Stemness of HFSCs in *Col17a1*-Null Skin

(A) Immunostaining of the dorsal skin from 8-week-old *Col17a1*$^{-/-}$ and from control mice with the IFE differentiation marker keratin 1 (KRT1) and Ki67. The bulge areas are demarcated by brackets. Top: In *Col17a1*$^{-/-}$ mice, cells coexpressing KRT15 (green) and KRT1 (red) appeared within the bulge area. Bottom: Cells in the bulge area of *Col17a1*$^{-/-}$ mice proliferated abnormally. As a control for anagen phase, dorsal skin at 5 days after hair-plucking of telogen follicles was used. Scale bar represents 50 μm.

(B) Loss of keratinocyte clonal growth potential resulting from *Col17a1* deficiency. (a) Clonal growth assays of keratinocytes from *Col17a1*$^{-/-}$ and from *Col17a1*$^{+/-}$ mice; representative dishes are shown. (b) *Col17a1*$^{-/-}$ keratinocytes formed only small colonies. (c) Colonies from *Col17a1*$^{-/-}$ skin were significantly fewer and smaller than those from *Col17a1*$^{+/-}$ control mice. *, **$p < 0.05$. (d) Keratinocytes from *Col17a1*$^{-/-}$ skin did not show decreased binding to 3T3-J2 feeder cells. $^{\#}p = 0.6653$, $^{\#\#}p = 0.162$.

See also Figure S4.

keratinocytes coexpress TGF-β1/2 in wild-type hair follicles (Figure 5F), demonstrating that HFSCs produce TGF-β1/2 in the bulge area. At 6 weeks of age, the expression of TGF-β1/2 was similar in bulge keratinocytes in the control and in *Col17a1*-null mice (Figure 5G). At 8 weeks of age or later, however, the hair follicle bulge exhibited significantly downregulated expression of TGF-β1/2 in *Col17a1*-null mice, although the hair follicle bulge in control mice showed a normal expression pattern (Figure 5G). Furthermore, phospho-Smad2 signals were not found either in bulge keratinocytes or in melanocytes of *Col17a1*-null mice but were present in control mice (Figure 5H). These findings demonstrate that niche features, including the loss of TGF-β1/2 production, are defective in *Col17a1*-null HFSCs. We reported previously that *Tgfbr2* (TGF-β receptor II) conditional knockout in mice via a bitransgenic system causes mild hair graying with incomplete penetrance (73.3% within 10 months after birth) possibly because of incomplete CRE-mediated recombination (Nishimura et al., 2010). In this study, we found that *Tgfbr2* straight knockout mice (with a *Rag2*-null background for the inhibition of multiorgan autoimmunity) show a severe hair graying phenotype with 100% penetrance within 5–6 weeks of age (Figure 5I). Thus, these data suggest that defective TGF-β signaling in MSCs resulting from the loss of TGF-β production from HFSCs affects MSC maintenance in *Col17a1* mutant mice and that HFSC-derived TGF-β signaling mediates the niche function of HFSCs for MSC maintenance.

Human COL17A1-Mediated Rescue of HFSCs Normalizes Maintenance of MSCs in *Col17a1*-Null Mice

Finally, to address whether the defects in *Col17a1*-null HFSCs induce the ectopic differentiation and eventual depletion of MSCs in the bulge area, leading to hair graying, we studied the impact of the transgenic rescue of *Col17a1*-null mice and in particular the HFSC phenotype resulting from forced expression of human *COL17A1* under control of the *Keratin 14* (*Krt14*) promoter (Olasz et al., 2007). In these rescued mice, human COL17A1 expression was restricted to basal keratinocytes and not to the melanocyte lineage (Figure S6A). As shown in Figure 6A, the hair coat of these mice was quite similar to that of *Col17a1*$^{+/-}$ mice and did not show progressive hair depigmentation or hair loss at 6 months of age, or even at 1 year of age (data not shown), whereas control *Col17a1*-null mice demonstrated the hair graying and other typical changes described above. Interestingly, both the distribution and morphology of *Dct-lacZ*-expressing melanoblasts in the bulge area were normal in the *Col17a1*$^{-/-}$*; Krt14-hCOL17A1* rescued mice (Figure 6B). Furthermore, the aberrant expression of Ki67 and KRT1, downregulation of TGF-β1/2 expression, and inactivation of TGF-β signaling in bulge keratinocytes were all also normalized (Figures 6C and 6D; Figure S6B). These findings demonstrate the dual critical roles of COL17A1 in HFSCs for their maintenance and for providing a niche for MSC maintenance through HFSC-derived TGF-β signaling (Figure 7).

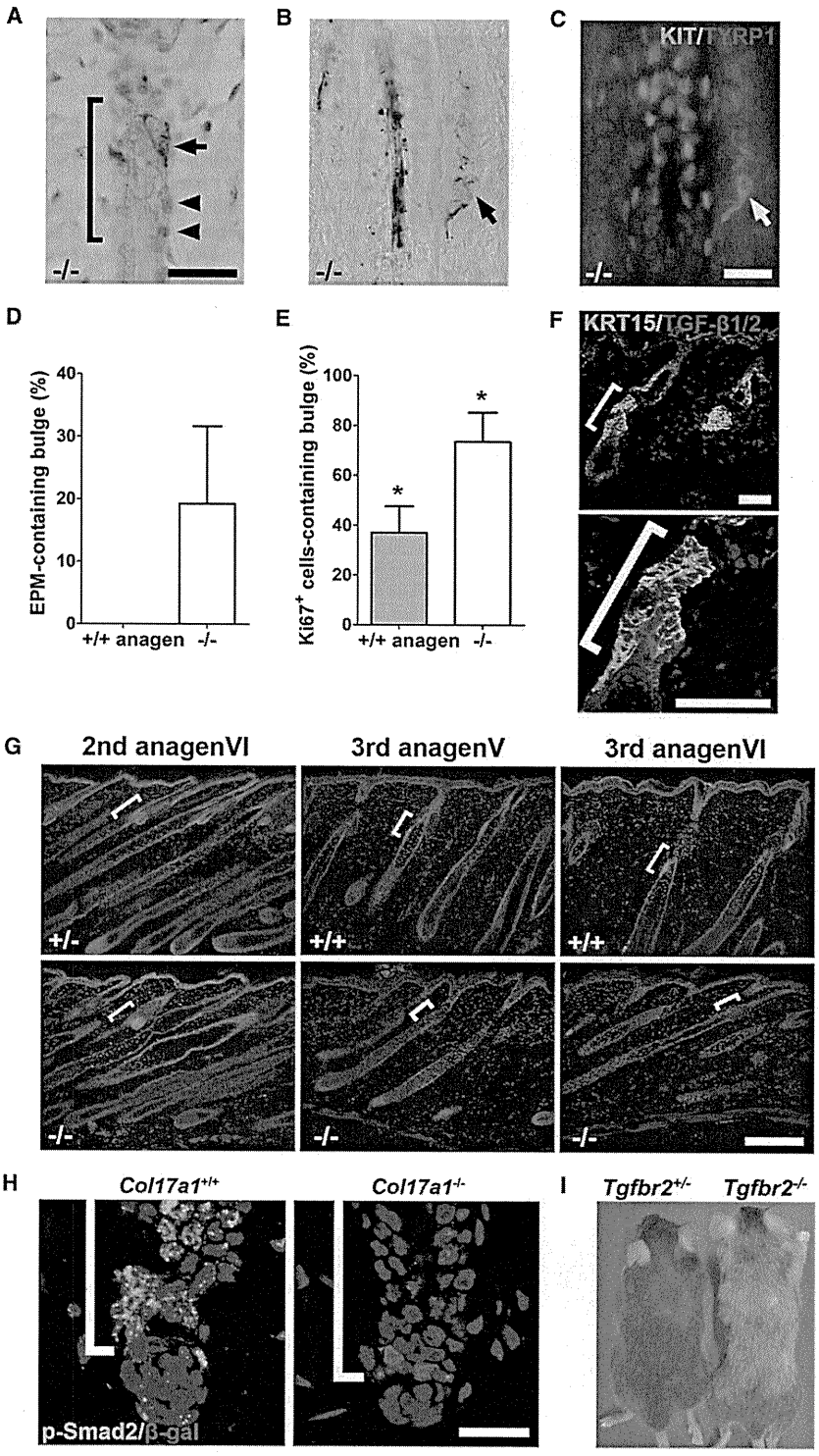

Figure 5. Ectopic Differentiation of MSCs in the Bulge Area with Diminished TGF-β Signaling Resulting from *Col17a1* Deficiency

(A–E) Ectopic differentiation of MSCs and surrounding keratinocytes in the bulge areas of *Col17a1*$^{-/-}$ follicles at 12 weeks of age. The bulge areas are demarcated by brackets. Ectopically pigmented melanocytes (A; arrow) are in direct contact with enlarged keratinocytes with large nuclei (A; arrowheads) in an anagen VI follicle; these ectopically pigmented melanocytes (arrow) are KIT^{+}/TYRP1^{+} cells with a dendritic morphology (B and C). Ectopically pigmented melanocytes were detected only in the bulge-subbulge area of *Col17a1*$^{-/-}$ follicles (D), and the proliferation of *Col17a1*$^{-/-}$ bulge keratinocytes at 12–13 weeks of age was abnormally accelerated compared with that of control anagen V follicles (E). *$p < 0.05$. Scale bars represent 30 μm in (A) and 20 μm in (B) and (C).

(F) Localization of TGF-β1/2 expression (red) in *Col17a1*$^{+/+}$ hair follicles. Plucked dorsal skins (4 days after hair plucking in telogen skin from 7-week-old *Col17a1*$^{+/+}$ mice) were used. KRT15-expressing keratinocytes (shown in green) express TGF-β1/2 (red). Scale bars represent 50 μm.

(G) *Col17a1*$^{-/-}$ mouse hair follicles from 5-week-old mice showed normal TGF-β1/2 expression patterns (left). However, at 8 weeks of age or later in *Col17a1*$^{-/-}$ mice, the TGF-β1/2 expression was downregulated (right and middle). Scale bar represents 200 μm.

(H) Phosphorylated Smad2 (shown in green) was not detected at 8 weeks in the *Col17a1*$^{-/-}$ hair follicle bulge. Dct-lacZ-expressing melanocytes in the bulge area are shown in red. Bulge areas are demarcated by brackets. Scale bar represents 20 μm.

(I) *Tgfbr2* straight knockout mice (*Tgfbr2* $^{-/-}$) (right) show severe hair graying phenotype at 6 weeks of age.

See also Figure S5.

DISCUSSION

Interactions between somatic stem cells and their surrounding niche microenvironment are critical for the establishment and maintenance of stem cell properties (Li and Xie, 2005; Moore and Lemischka, 2006). Although previous in vitro studies suggested some correlation in keratinocytes between integrin-mediated extracellular matrix adhesion and proliferation potential, in vivo ablation studies of major integrins in basal keratinocytes have not provided data on stem cell-specific depletion phenotypes (Dowling et al., 1996; Georges-Labouesse et al., 1996; Raghavan et al., 2000; van der Neut et al., 1996; Watt, 2002). In the present study, we demonstrated that COL17A1, a hemidesmosomal transmembrane collagen, is highly expressed in HFSCs within hair follicles and is required for the self-renewal of HFSCs. We found that *Col17a1* ablation in mice results in premature hair loss almost homogeneously over the entire body surface without showing any specific association

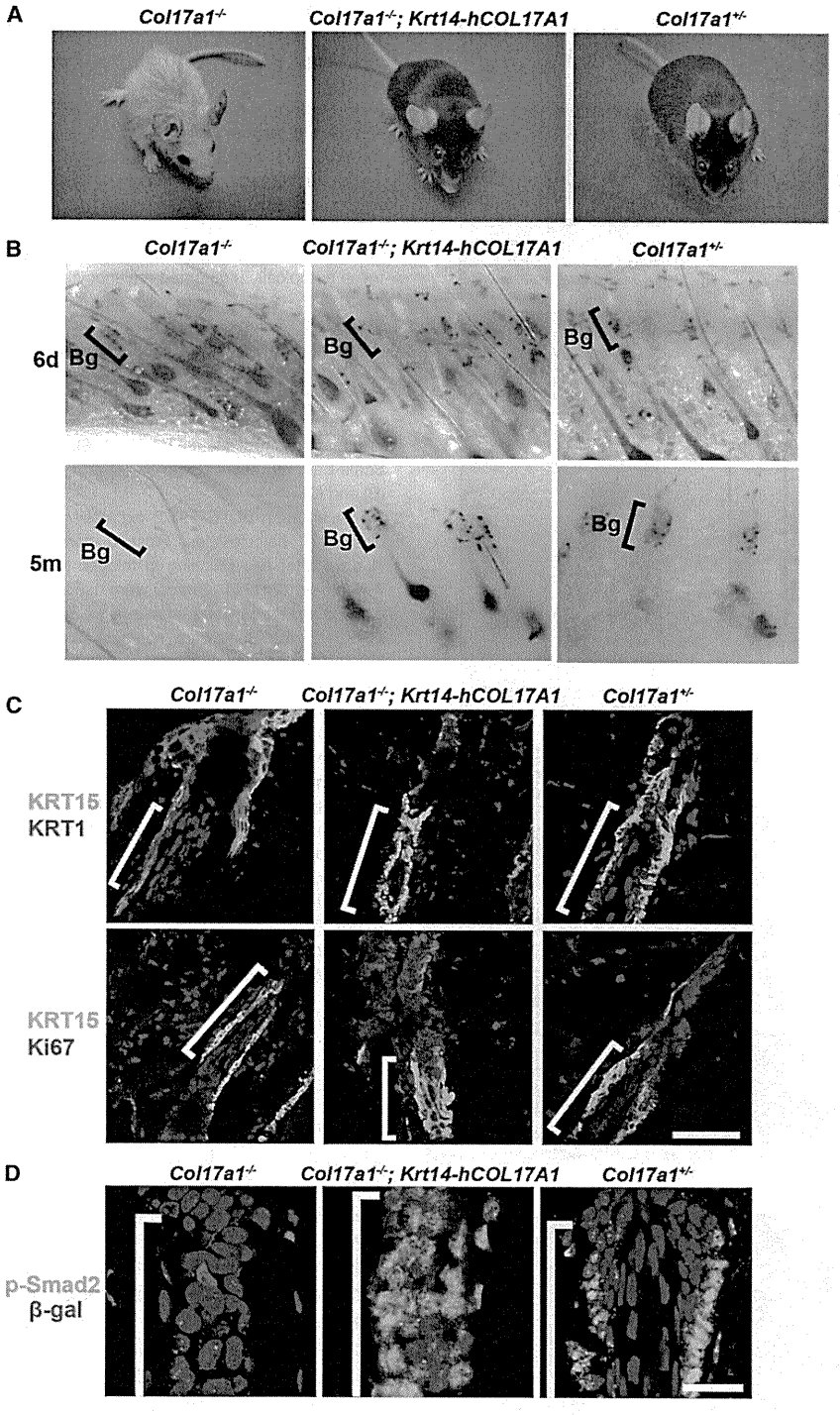

Figure 6. Transgene-Mediated Correction of *COL17A1* Expression in *Col17a1*$^{-/-}$ Basal Keratinocytes Rescues the Loss of MSCs

The *Krt14-hCOL17A1* transgene was introduced into *Col17a1*$^{-/-}$ mice.

(A) Macroscopic phenotype of 7- to 9-month-old *Col17a1*$^{-/-}$ mice with the *Krt14-hCOL17A1* transgene and *Col17a1*$^{+/-}$ mice.

(B) Distribution and morphology of *Dct-lacZ*-expressing melanoblasts in the bulge area (Bg) are normalized by the *Krt14-hCOL17A1* transgene in *Col17a1*$^{-/-}$ mice. Bulge-subbulge areas are demarcated by brackets.

(C) Ectopic KRT1 expression and abnormal proliferation of HFSCs in the bulge-subbulge area (brackets) are corrected by the *Krt14-hCOL17A1* transgene in *Col17a1*$^{-/-}$ mice. These mice were observed at 13 weeks of age during the anagen phase. Scale bar represents 50 μm.

(D) The downregulated expression of phospho-Smad2 (in green) in *Col17a1*$^{-/-}$ HFSCs and MSCs within the bulge-subbulge areas (demarcated by brackets) was also normalized by forced expression of the *Krt14-hCOL17A1* transgene in *Col17a1*$^{-/-}$ keratinocytes. Dct-lacZ-expressing melanocytes in the bulge area are shown in red. Scale bars represents 20 μm.

See also Figure S6.

with mechanical stress. Although mechanical stress, such as attempts to peel the neonatal mouse skin, can induce skin erosion or blistering in *Col17a1*-null mice (Nishie et al., 2007), it did not significantly accelerate hair graying or hair loss in these mice. Importantly, we did not find evidence of macroscopic/microscopic junctional separation, basal cell death, nor inflammatory cell infiltrates between the HFSCs and the basement membrane in *Col17a1*-null mouse skin. Instead, we found that significant defects in HFSC quiescence and immaturity in *Col17a1*-null mice were the earliest events that could explain the defective maintenance of HFSCs over ensuing hair cycles. These findings underline a critical cell-autonomous role for COL17A1 in the maintenance of HFSCs under physiological conditions. Although we did not detect adhesion defects of *Col17a1*-null keratinocytes on feeder cells used for colony assay in this study, weakening of cell attachment has been found with human cultured keratinocytes treated with COL17A1 antibody under vibration conditions (Iwata et al., 2009). One adhesion-based explanation for the premature HFSC depletion in *Col17a1*-deficient mice is that COL17A1-dependent anchoring of HFSCs to the basal lamina might regulate the quiescence and differentiation of HFSCs by modifying their division frequency and properties. Regardless of the precise mechanism involved, our findings reveal a potential mechanism for the hair loss (alopecia) seen with human *COL17A1* deficiency, which causes the nonlethal form of junctional epidermolysis bullosa, also known as generalized atrophic benign epidermolysis bullosa (GABEB) (McGrath et al., 1995; Nishie et al., 2007). It has been reported that the hair loss in GABEB patients is not always associated with

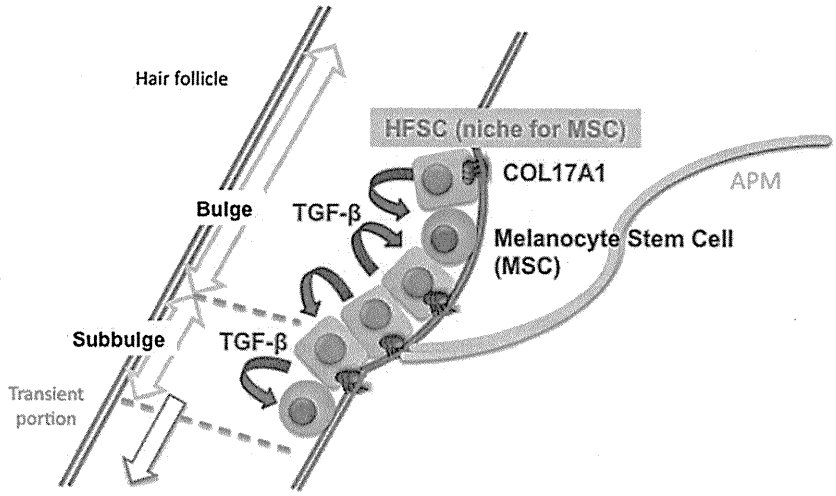

Figure 7. A Schematic Model for HFSCs and MSC Niche
HFSCs provide COL17A1-dependent niche for MSCs though TGF-β signaling. APM, arrector pili muscle.

surrounding skin surface changes but is associated with hair follicle atrophy or hair follicle loss (Hintner and Wolff, 1982). This finding is consistent with the late skin changes such as hair follicle atrophy seen in *Col17a1*-null mice. Therefore, we suggest that this mouse model may be a powerful tool for helping to understand the pathomechanisms of premature alopecia.

Human patients with GABEB also show epidermal atrophy with aging. *Col17a1*-deficient mice show transient epidermal hyperplasia in some focal areas at around 6 months of age (Figure 3D) but the entire skin becomes gradually more atrophic over time. Similar but more pronounced changes have been observed in the setting of stem cell depletion such as is seen in *Rac1* conditional knockout mice (Benitah et al., 2005) and in c-Myc transgenic mice (Arnold and Watt, 2001; Waikel et al., 2001). The late onset of epidermal atrophy seen in *Col17a1*-null mice might represent the eventual depletion or a decreased self-renewing potential of epidermal stem cells for the IFE.

More generally, *Col17a1*-null mice have provided evidence of an unexpected biological function for HFSCs. Although we have previously shown that the niche microenvironment plays a dominant role in fate determination for MSCs (Nishimura et al., 2002), the type of cell and/or the extracellular matrix in the bulge area that comprises the functionally essential component(s) of the niche has been unclear. Our current data indicate that HFSCs serve as a functional niche for MSCs and act through HFSC-derived TGF-β signaling, which is critical for MSC maintenance (Figure 7). It is notable that MSC immaturity was lost in *Col17a1*-deficient mice at a time when HFSCs were undergoing aberrant proliferation and differentiation in the bulge area with gradual loss of HFSC characteristics, including TGF-β production. There are a number of keratinocyte-specific gene-deficient mice that display a hair loss phenotype caused by HFSC depletion (Benitah et al., 2005; Zanet et al., 2005). However, as far as we know, characteristic premature hair graying has not been reported in those mice. It is also interesting that HFSCs nurture MSCs even though they are derived from a completely different developmental origin (Nishimura et al., 1999, 2002). A similar niche function provided by one type of stem cell for another was reported in *Drosophila melanogaster* testis and mouse bone marrow during the revision of this paper (Leatherman and Dinardo, 2010; Méndez-Ferrer et al., 2010; Omatsu et al., 2010). The maintenance of somatic stem cell populations in a coherent cell mass with a specialized tissue organization such as in the hair follicle bulge might be a recurring strategy for somatic stem cell maintenance. COL17A1 in the basal cell population of HFSCs (the α6-integrin^{high} population) (Blanpain et al., 2004) is critical not only for the maintenance of MSCs but also for the suprabasal HFSCs (α6-integrin^{low} population), which suggests a common niche function for basal HFSCs for the maintenance of adjacent MSCs and HFSCs. Further studies to elucidate the precise niche properties of HFSCs may clarify additional fundamental mechanisms for the maintenance of stem cell pools as clustered stem cell populations.

EXPERIMENTAL PROCEDURES

Animals

Dct-lacZ transgenic mice (Mackenzie et al., 1997) (a gift from I. Jackson), *Col17a1*-knockout mice (Nishie et al., 2007), and *Krt14*-human *COL17A1* transgenic mice (Olasz et al., 2007) have been described previously. *Col17a1*$^{+/+}$ and *Col17a1*$^{+/-}$ mice are referred to as control mice. *CAG-CAT-EGFP* mice (a gift from J. Miyazaki) were bred with *Dct*$^{tml(Cre)Bee}$ mice (a gift from F. Beermann) to generate compound heterozygotes as described previously (Osawa et al., 2005). All mice were backcrossed to C57BL/6J. Animal experiments conformed to the Guide for the Care and Use of Laboratory Animals and were approved by the Institutional Committee of Laboratory Animal Experimentation.

TGF-βRII straight knockout mice (a gift from M. Taketo) (Oshima et al., 1996) were bred with Rag2-deficient mice at the Animal Research Facility of the Institute of Medical Science, University of Tokyo. Animal care of the line was carried out in accordance with the guidance of Tokyo University for animal and recombinant DNA experiments.

Histology, Immunohistochemistry, and Flow Cytometry Analyses

Paraffin, frozen sections, and whole-mount β-galactosidase staining were performed as previously described (Nishimura et al., 2002, 2005). Additional details on the methods and antibodies used are provided in the Supplemental Information. Multicolor flow cytometry analysis for HFSCs was performed with a FACSCalibur (BD).

Electron Microscopy

For electron microscopy, 20 μm cryostat sections were cut and stained in X-gal solution for 12 hr at 37°C. The sections were postfixed in 0.5% osmium tetroxide for 30 min, stained with 1% uranyl acetate for 20 min, dehydrated in a graded ethanol series, and then embedded in epoxy resin. Semithin sections (1 μm thick) were examined after toluidine blue staining and were observed by light microscopy. Ultrathin sections were observed with a JEM-1210 transmission electron microscope (JEOL) at 80 KV.

Isolation of Melanocytes

Dorsal skin was harvested from 6-day-old *CAG-CAT-EGFP/+; Dct$^{tml(Cre)Bee/\ tml(Cre)Bee}$* mice. The skin specimens were incubated in PBS containing 300 U/ml dispase (Sanko Junyaku) overnight at 4°C, and then the dermis was removed from the epidermis with a stereomicroscope. The epidermis was further dissociated by treatment with 0.25% trypsin for 10 min at 37°C. After neutralization with fetal calf serum (FCS), GFP$^+$ melanocytes were sorted with JSAN (Bay Bioscience).

RNA Isolation and Reverse Transcriptase Polymerase Chain Reaction

Total RNAs from mouse skin or sorted GFP$^+$ melanocytes were isolated with TRIzol (GIBCO) according to the manufacturer's instructions. 3 μg total RNA was used for cDNA synthesis in THERMOSCRIPT RT-PCR System (GIBCO) according to the manufacturer's instructions. The following primers were used for the analysis: mouse *Col17a1* (forward primer 5′-actcgcctcttcttca acca, reverse primer 5′-gagcaggacgccatgttatt) and *GAPDH* (forward primer 5′-accacagtccatgccatcac, reverse primer 5′-tccaccaccctgttgctgta).

Colony-Formation and Adhesion Assays

For the colony-forming assay, keratinocytes from newborn mice were used. Dorsal skins were incubated in PBS containing 300 U/ml dispase (Sanko Junyaku) for 1 hr at 37°C, after which the dermis was removed from the epidermis with a stereomicroscope. The epidermis was further dissociated by treatment with TrypLE Select (GIBCO) for 10 min at 37°C. The isolated cells (10^5 per 6 cm dish) were seeded on 3T3-J2 feeder cells treated with mitomycin C. The cells were grown in calcium-free medium (3:1 = calcium-free DMEM:CnT-57CF.S [Celltec]) supplemented with 1.8×10^{-4} M adenine, 1% antibiotic-antimyotic solution (Sigma), 2 mM L-glutamine, 0.5 μg/ml hydrocortisone, 5 μg/ml insulin, 10^{-10} M cholera enterotoxin, 10 ng/ml EGF, and 10% FCS treated with Chelex-100 resin (BioRad) at 32°C in a humidified atmosphere with 8% CO_2 for a total of 14 days. To visualize the keratinocyte colonies, the cells were washed with PBS and were then fixed in 4% formalin for 20 min at room temperature. After further washing in PBS, the cultures were stained for 5 min at room temperature with crystal violet.

For the adhesion assay, isolated keratinocytes (10^5 per well in 6-well plates) were seeded on 3T3-J2 feeder cells treated with mitomycin C or on collagen I-coated 6-well plates. 12 or 24 hr later, keratinocytes was washed three times in PBS and were collected with 0.05% trypsin-EDTA. Collected cells were fixed with 2% formaldehyde for 10 min at 37°C, permeabilized by ice-cold 100% methanol for 30 min, and stained with an Alexa Fluor 488-conjugated pan-cytokeratin monoclonal antibody (EXBIO). Detection of adherent keratinocytes was performed with a FACSCanto II (BD).

SUPPLEMENTAL INFORMATION

Supplemental Information includes Supplemental Experimental Procedures and six figures and can be found with this article online at doi:10.1016/j.stem.2010.11.029.

ACKNOWLEDGMENTS

We thank Dr. Makoto Taketo for *Tgfbr2* knockout mice; Dr. Hideki Nakamura, Dr. Tomohiko Wakayama, and Dr. Shoichi Iseki for their technical advice concerning electron microscopic analysis; Dr. Hiroyuki Nishimura for critical reading of the manuscript; Dr. Masashi Akiyama for discussion; Dr. Atsushi Hirao and Dr. Masako Ohmura for the use of the flow cytometer; Dr. Ken Natsuga and Ms. Kaori Sakai for sample identification; and Ms. Misa Suzuki, Ms. Megumi Sato, and Ms. Yuika Osaki for technical assistance. This study was supported by grants from the Japanese Ministry of Education, Culture, Sports, Science, and Technology (17689033, 19390293), the Uehara Memorial Foundation, the Kato Memorial Bioscience Foundation, and the Takeda Science Foundation to E.K.N.

Received: May 13, 2009
Revised: July 27, 2010
Accepted: October 23, 2010
Published: February 3, 2011

REFERENCES

Arnold, I., and Watt, F.M. (2001). c-Myc activation in transgenic mouse epidermis results in mobilization of stem cells and differentiation of their progeny. Curr. Biol. *11*, 558–568.

Barrandon, Y., and Green, H. (1987). Three clonal types of keratinocyte with different capacities for multiplication. Proc. Natl. Acad. Sci. USA *84*, 2302–2306.

Benitah, S.A., Frye, M., Glogauer, M., and Watt, F.M. (2005). Stem cell depletion through epidermal deletion of Rac1. Science *309*, 933–935.

Blanpain, C., and Fuchs, E. (2006). Epidermal stem cells of the skin. Annu. Rev. Cell Dev. Biol. *22*, 339–373.

Blanpain, C., Lowry, W.E., Geoghegan, A., Polak, L., and Fuchs, E. (2004). Self-renewal, multipotency, and the existence of two cell populations within an epithelial stem cell niche. Cell *118*, 635–648.

Cotsarelis, G. (2006). Epithelial stem cells: A folliculocentric view. J. Invest. Dermatol. *126*, 1459–1468.

Darling, T.N., Bauer, J.W., Hintner, H., and Yancey, K.B. (1997). Generalized atrophic benign epidermolysis bullosa. Adv. Dermatol. *13*, 87–119, , discussion 120.

Dowling, J., Yu, Q.C., and Fuchs, E. (1996). Beta4 integrin is required for hemidesmosome formation, cell adhesion and cell survival. J. Cell Biol. *134*, 559–572.

Georges-Labouesse, E., Messaddeq, N., Yehia, G., Cadalbert, L., Dierich, A., and Le Meur, M. (1996). Absence of integrin alpha 6 leads to epidermolysis bullosa and neonatal death in mice. Nat. Genet. *13*, 370–373.

Greco, V., Chen, T., Rendl, M., Schober, M., Pasolli, H.A., Stokes, N., Dela Cruz-Racelis, J., and Fuchs, E. (2009). A two-step mechanism for stem cell activation during hair regeneration. Cell Stem Cell *4*, 155–169.

Green, H. (1977). Terminal differentiation of cultured human epidermal cells. Cell *11*, 405–416.

Guasch, G., Schober, M., Pasolli, H.A., Conn, E.B., Polak, L., and Fuchs, E. (2007). Loss of TGFbeta signaling destabilizes homeostasis and promotes squamous cell carcinomas in stratified epithelia. Cancer Cell *12*, 313–327.

Hintner, H., and Wolff, K. (1982). Generalized atrophic benign epidermolysis bullosa. Arch. Dermatol. *118*, 375–384.

Hojiro, O. (1972). Fine structure of the mouse hair follicle. J. Electron Microsc. (Tokyo) *21*, 127–138.

Inomata, K., Aoto, T., Binh, N.T., Okamoto, N., Tanimura, S., Wakayama, T., Iseki, S., Hara, E., Masunaga, T., Shimizu, H., and Nishimura, E.K. (2009). Genotoxic stress abrogates renewal of melanocyte stem cells by triggering their differentiation. Cell *137*, 1088–1099.

Iwata, H., Kamio, N., Aoyama, Y., Yamamoto, Y., Hirako, Y., Owaribe, K., and Kitajima, Y. (2009). IgG from patients with bullous pemphigoid depletes cultured keratinocytes of the 180-kDa bullous pemphigoid antigen (type XVII collagen) and weakens cell attachment. J. Invest. Dermatol. *129*, 919–926.

Leatherman, J.L., and Dinardo, S. (2010). Germline self-renewal requires cyst stem cells and stat regulates niche adhesion in *Drosophila* testes. Nat. Cell Biol. *12*, 806–811.

Li, L., and Xie, T. (2005). Stem cell niche: Structure and function. Annu. Rev. Cell Dev. Biol. *21*, 605–631.

Mackenzie, M.A., Jordan, S.A., Budd, P.S., and Jackson, I.J. (1997). Activation of the receptor tyrosine kinase Kit is required for the proliferation of melanoblasts in the mouse embryo. Dev. Biol. *192*, 99–107.

Masunaga, T., Shimizu, H., Yee, C., Borradori, L., Lazarova, Z., Nishikawa, T., and Yancey, K.B. (1997). The extracellular domain of BPAG2 localizes to anchoring filaments and its carboxyl terminus extends to the lamina densa of normal human epidermal basement membrane. J. Invest. Dermatol. *109*, 200–206.

McGrath, J.A., Gatalica, B., Christiano, A.M., Li, K., Owaribe, K., McMillan, J.R., Eady, R.A., and Uitto, J. (1995). Mutations in the 180-kD bullous pemphigoid antigen (BPAG2), a hemidesmosomal transmembrane collagen (COL17A1), in generalized atrophic benign epidermolysis bullosa. Nat. Genet. *11*, 83–86.

McMillan, J.R., Akiyama, M., and Shimizu, H. (2003). Epidermal basement membrane zone components: Ultrastructural distribution and molecular interactions. J. Dermatol. Sci. *31*, 169–177.

Méndez-Ferrer, S., Michurina, T.V., Ferraro, F., Mazloom, A.R., Macarthur, B.D., Lira, S.A., Scadden, D.T., Ma'ayan, A., Enikolopov, G.N., and Frenette, P.S. (2010). Mesenchymal and haematopoietic stem cells form a unique bone marrow niche. Nature *466*, 829–834.

Moore, K.A., and Lemischka, I.R. (2006). Stem cells and their niches. Science *311*, 1880–1885.

Morris, R.J., Liu, Y., Marles, L., Yang, Z., Trempus, C., Li, S., Lin, J.S., Sawicki, J.A., and Cotsarelis, G. (2004). Capturing and profiling adult hair follicle stem cells. Nat. Biotechnol. *22*, 411–417.

Nishie, W., Sawamura, D., Goto, M., Ito, K., Shibaki, A., McMillan, J.R., Sakai, K., Nakamura, H., Olasz, E., Yancey, K.B., et al. (2007). Humanization of autoantigen. Nat. Med. *13*, 378–383.

Nishimura, E.K., Yoshida, H., Kunisada, T., and Nishikawa, S.I. (1999). Regulation of E- and P-cadherin expression correlated with melanocyte migration and diversification. Dev. Biol. *215*, 155–166.

Nishimura, E.K., Jordan, S.A., Oshima, H., Yoshida, H., Osawa, M., Moriyama, M., Jackson, I.J., Barrandon, Y., Miyachi, Y., and Nishikawa, S. (2002). Dominant role of the niche in melanocyte stem-cell fate determination. Nature *416*, 854–860.

Nishimura, E.K., Granter, S.R., and Fisher, D.E. (2005). Mechanisms of hair graying: Incomplete melanocyte stem cell maintenance in the niche. Science *307*, 720–724.

Nishimura, E.K., Suzuki, M., Igras, V., Du, J., Lonning, S., Miyachi, Y., Roes, J., Beermann, F., and Fisher, D.E. (2010). Key roles for transforming growth factor beta in melanocyte stem cell maintenance. Cell Stem Cell *6*, 130–140.

Nishizawa, Y., Uematsu, J., and Owaribe, K. (1993). HD4, a 180 kDa bullous pemphigoid antigen, is a major transmembrane glycoprotein of the hemidesmosome. J. Biochem. *113*, 493–501.

Nowak, J.A., Polak, L., Pasolli, H.A., and Fuchs, E. (2008). Hair follicle stem cells are specified and function in early skin morphogenesis. Cell Stem Cell *3*, 33–43.

Olasz, E.B., Roh, J., Yee, C.L., Arita, K., Akiyama, M., Shimizu, H., Vogel, J.C., and Yancey, K.B. (2007). Human bullous pemphigoid antigen 2 transgenic skin elicits specific IgG in wild-type mice. J. Invest. Dermatol. *127*, 2807–2817.

Omatsu, Y., Sugiyama, T., Kohara, H., Kondoh, G., Fujii, N., Kohno, K., and Nagasawa, T. (2010). The essential functions of adipo-osteogenic progenitors as the hematopoietic stem and progenitor cell niche. Immunity *33*, 387–399.

Osawa, M., Egawa, G., Mak, S.S., Moriyama, M., Freter, R., Yonetani, S., Beermann, F., and Nishikawa, S. (2005). Molecular characterization of melanocyte stem cells in their niche. Development *132*, 5589–5599.

Oshima, M., Oshima, H., and Taketo, M.M. (1996). TGF-beta receptor type II deficiency results in defects of yolk sac hematopoiesis and vasculogenesis. Dev. Biol. *179*, 297–302.

Oshima, H., Rochat, A., Kedzia, C., Kobayashi, K., and Barrandon, Y. (2001). Morphogenesis and renewal of hair follicles from adult multipotent stem cells. Cell *104*, 233–245.

Paus, R., and Cotsarelis, G. (1999). The biology of hair follicles. N. Engl. J. Med. *341*, 491–497.

Paus, R., Müller-Röver, S., Van Der Veen, C., Maurer, M., Eichmüller, S., Ling, G., Hofmann, U., Foitzik, K., Mecklenburg, L., and Handjiski, B. (1999). A comprehensive guide for the recognition and classification of distinct stages of hair follicle morphogenesis. J. Invest. Dermatol. *113*, 523–532.

Powell, A.M., Sakuma-Oyama, Y., Oyama, N., and Black, M.M. (2005). Collagen XVII/BP180: a collagenous transmembrane protein and component of the dermoepidermal anchoring complex. Clin. Exp. Dermatol. *30*, 682–687.

Qiao, W., Li, A.G., Owens, P., Xu, X., Wang, X.J., and Deng, C.X. (2006). Hair follicle defects and squamous cell carcinoma formation in Smad4 conditional knockout mouse skin. Oncogene *25*, 207–217.

Raghavan, S., Bauer, C., Mundschau, G., Li, Q., and Fuchs, E. (2000). Conditional ablation of beta1 integrin in skin. Severe defects in epidermal proliferation, basement membrane formation, and hair follicle invagination. J. Cell Biol. *150*, 1149–1160.

Raymond, K., Deugnier, M.A., Faraldo, M.M., and Glukhova, M.A. (2009). Adhesion within the stem cell niches. Curr. Opin. Cell Biol. *21*, 623–629.

Tumbar, T., Guasch, G., Greco, V., Blanpain, C., Lowry, W.E., Rendl, M., and Fuchs, E. (2004). Defining the epithelial stem cell niche in skin. Science *303*, 359–363.

van der Neut, R., Krimpenfort, P., Calafat, J., Niessen, C.M., and Sonnenberg, A. (1996). Epithelial detachment due to absence of hemidesmosomes in integrin beta 4 null mice. Nat. Genet. *13*, 366–369.

Waikel, R.L., Kawachi, Y., Waikel, P.A., Wang, X.J., and Roop, D.R. (2001). Deregulated expression of c-Myc depletes epidermal stem cells. Nat. Genet. *28*, 165–168.

Watt, F.M. (2002). Role of integrins in regulating epidermal adhesion, growth and differentiation. EMBO J. *21*, 3919–3926.

Yang, L., Mao, C., Teng, Y., Li, W., Zhang, J., Cheng, X., Li, X., Han, X., Xia, Z., Deng, H., and Yang, X. (2005). Targeted disruption of Smad4 in mouse epidermis results in failure of hair follicle cycling and formation of skin tumors. Cancer Res. *65*, 8671–8678.

Yang, L., Wang, L., and Yang, X. (2009). Disruption of Smad4 in mouse epidermis leads to depletion of follicle stem cells. Mol. Biol. Cell *20*, 882–890.

Zanet, J., Pibre, S., Jacquet, C., Ramirez, A., de Alborán, I.M., and Gandarillas, A. (2005). Endogenous Myc controls mammalian epidermal cell size, hyperproliferation, endoreplication and stem cell amplification. J. Cell Sci. *118*, 1693–1704.

Hair Shaft Abnormalities in Localized Autosomal Recessive Hypotrichosis 2 and A Review of Other Non-syndromic Human Alopecias

Hiraku Suga[1], Yuichiro Tsunemi[1], Makoto Sugaya[1], Satoru Shinkuma[2], Masashi Akiyama[2], Hiroshi Shimizu[2] and Shinichi Sato[1]
Departments of Dermatology, [1]Faculty of Medicine, University of Tokyo, 7-3-1 Hongo, Bunkyo-ku, Tokyo 113-8655, and [2]Hokkaido University Graduate School of Medicine, Sapporo, Japan. E-mail: hiraku_s2002@yahoo.co.jp
Accepted December 16, 2010.

Localized autosomal recessive hypotrichosis (LAH) 2 is a type of non-syndromic human alopecia that is inherited as an autosomal recessive trait. We describe here a patient with LAH2 who had mutations in the *lipase H* (*LIPH*) gene. We analysed hair shaft morphology using light and scanning electron microscopy (SEM). In addition, we review the features of other non-syndromic human alopecias.

CASE REPORT

The patient was a 4-year-old boy, the firstborn of healthy and unrelated Japanese parents, born after an uneventful pregnancy. He had scant hair at birth, which grew very slowly in infancy.

Clinical examination revealed hypotrichosis of the scalp (Fig. 1a). The hairs were sparse, thin, and curly, and not easily plucked. The left eyebrow hair was sparse, but the eyelashes and other body hair were present in normal amounts. Teeth, nails, and the ability to sweat were completely normal. Clinical features of keratosis pilaris, milia, scarring, and palmoplantar keratoderma were absent. Psychomotor development was normal. The patient's younger brother also had severe hypotrichosis; since birth his hair was curly, and his eyebrow hair virtually absent (Fig. 1b). No other family members, including his parents, had similar hair abnormalities. Laboratory tests of the patient showed normal serum levels of copper and zinc, and liver and kidney function tests were all within normal ranges. Over a period of 2 years there was no improvement or exacerbation of hypotrichosis in the patient.

Light microscopy of the patient's scalp hairs revealed that approximately 10% had structural abnormalities. Abnormal hairs were composed of thick dark parts and thin light parts (Fig. 2a). SEM revealed alterations of the cuticular architecture. Cuticular cells were absent from both the thick and thin parts (Fig. 2b). Cross-sectional observation showed that thick, but not thin, sections had hair medulla (Fig. 2c, d). Light microscopy on hairs from the patient's younger brother revealed that they were composed of thin and thick parts (data not shown).

Based on the clinical features, hair microscopy and family pedigree, we suspected LAH2 or LAH3. To determine the type of LAH, we looked for gene mutations in *LIPH* and *LPAR6* (encoding lysophosphatidic acid receptor 6). Two prevalent missense mutations in *LIPH* were found (1); c.736T>A (p.Cys246Ser) and c.742C>A (p.His248Asn). The mutations were carried in a compound heterozygous state. No mutations were found in *LPAR6*. The parents did not consent to genetic testing of the younger brother or themselves.

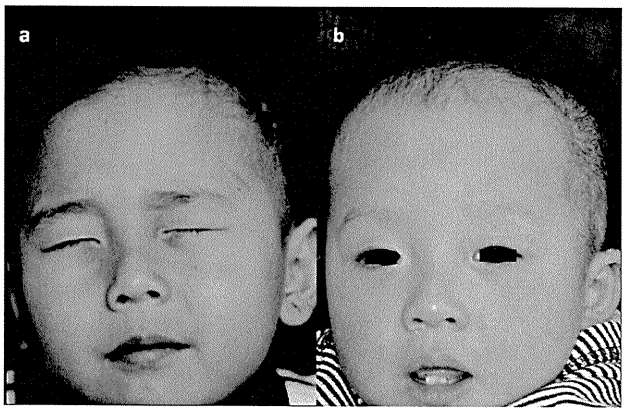

Fig. 1. (a) Clinical features of the patient at 4 years of age. (b) Clinical features of the younger brother at 1 year 4 months of age. Permission is given from the parents to publish these photos.

DISCUSSION

The different LAH subtypes map to chromosomes 18q12.1, 3q27.3 and 13q14.11–13q21.32, and are designated LAH1, LAH2 and LAH3, respectively (2–4). Mutations in *DSG4* (encoding desmoglein 4) have been found to be responsible for LAH1 (5). Kazantseva et al. (6) reported deletion mutations in *LIPH* leading to LAH2. Pasternack et al. (7) reported disruption of *LPAR6* in families affected with LAH3.

Table I summarizes of genetic, non-syndromic human alopecias. In *hypotrichosis simplex of the scalp*, hair loss

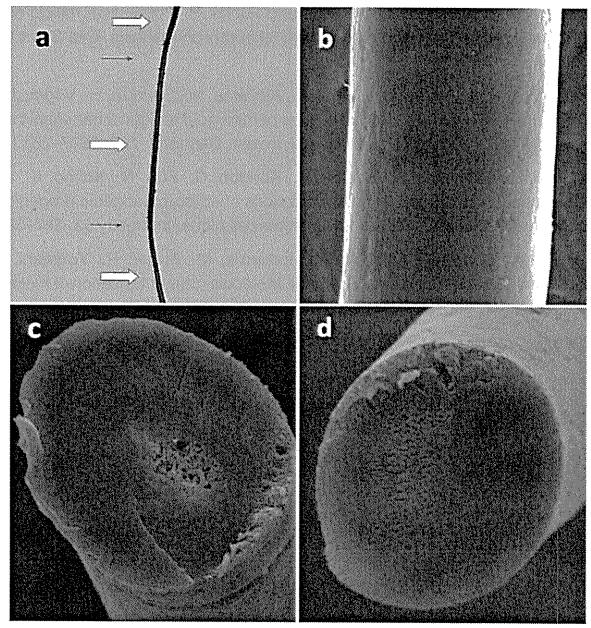

Fig. 2. (a) Light microscopy (×40). Hair was composed of thick (⇨) and thin parts (→). (b) Scanning electron microscopy (×900). Cuticular cells were absent in both thick and thin sections. (c, d) Scanning electron microscopy (cross-section, ×900). (c) Thick regions showed hair medulla, while (d) thin regions did not.

is limited to the scalp without hair shaft abnormalities. The causative gene is *CDSN* (encoding corneodesmosin) on 6p21.3 (8). The clinical presentations of *monilethrix* vary among patients. Mild cases have hair loss limited to the scalp, while severe cases show generalized alopecia. Hair shaft abnormalities are characteristic, demonstrating regularly-spaced, spindle-shaped swellings. The nodes are as thick as normal hair and the atrophic internodes represent areas where the hair is easily broken. Causative genes are *hHb1*, *hHb3* and *hHb6* (12q13) (9), which encode for basic hair keratins.

In case of *atrichia with papular lesions*, hair loss on the entire body occurs several months after birth. The gene responsible is *HR* (encoding "hairless") (10), a transcription modulating factor that influences the regression phase of the hair shaft cycle. Patients with *hypotrichosis, Marie Unna type* have hard and rough scalp hair, described as iron-wire hair. Generalized hypotrichosis is often seen. *U2HR*, an inhibitory upstream open reading frame of the human hairless gene (11), is mutated in this condition. *Hereditary hypotrichosis simplex* is characterized by hair follicle miniaturization. The defective gene is *APCDD1* (encoding adenomatosis polyposis down-regulated 1) (12). Hairs are short, thin, and easily plucked. Eyelashes and eyebrows are also affected.

As already mentioned, there are three types of *localized hereditary hypotrichosis*. LAH1 patients have hair shaft abnormalities that resemble moniliform hair (13). LAH1 can be viewed as an autosomal recessive form of monilethrix. Patients with LAH2 and LAH3 have woolly hair (14, 15), and eyelashes and eyebrows are often sparse or absent. Upper and lower limb hairs are sometimes absent too.

Our patient had hypotrichosis of the scalp with sparse left eyebrow hair and irregularly spaced segments of thick and thin hair, but not to a degree that could be labelled moniliform. The mode of inheritance was autosomal recessive and *LIPH* was found to be abnormal, thus establishing a diagnosis of LAH2. One of the mutations (c.736T>A) leads to an amino acid change (p.Cys246Ser) of a conserved cysteine residue, which forms intramolecular disulphide bonds in the lid domain in the structure model of LIPH (1). The other mutation (c.742C>A) results in alteration of one of the amino acids of the catalytic triad (Ser^{154}, Asp^{178}, and His^{248}) of LIPH (p.His248Asn) (1).

Regarding hair shaft morphology, Horev et al. (14) reported that hairs of LAH2 patients showed decreased diameter under light microscopy. This is the first report to describe hairs from an LAH2 patient by SEM. Shimomura et al. (13) observed hairs of LAH1 patients by SEM and found variable thickness of the hair shaft, resulting in nodes and internodes. Which are absent in LAH1 (our observation). Longitudinal ridges and flutes were observed at internodes, and the breaks always occurred at internodes in LAH1. These features resemble those of moniliform hair rather than LAH2. However, in the end gene analysis is probably easier to accomplish than SEM to distinguish the two types of LAH.

ACNOWLEDGEMENTS

We thank Dr Andrew Blauvelt, Department of Dermatology, Oregon Health & Science University, for many helpful comments.

REFERENCES

1. Shinkuma S, Akiyama M, Inoue A, Aoki J, Natsuga K, Nomura T, et al. LIPH prevalent founder mutations lead to loss of P2Y5 activation ability of PA-PLA1α in autosomal recessive hypotrichosis. Hum Mutat 2010; 31: 602–610.
2. Rafique MA, Ansar M, Jamai SM, Malik S, Sohail M, Faiyaz-Ul-Haque M, et al. A locus for hereditary hypotrichosis localized to human chromosome 18q21.1. Eur J Hum Genet 2003; 11: 623–628.
3. Aslam M, Chahrour MH, Razzaq A, Haque S, Yan K, Leal SM, et al. A novel locus for autosomal recessive form of hypotrichosis maps to chromosome 3q26.33-q27.3. J Med Genet 2004; 41: 849–852.
4. Wali A, Chishti MS, Ayub M, Yasinzai M, Kafaitullah, Ali G, et al. Localization of a novel autosomal recessive hypotrichosis locus (LAH3) to chromosome 13q14.11-q21.32. Clin Genet 2007; 72: 23–29.
5. Kljuic A, Bazzi H, Sundberg JP, Martinez-Mir A, O'Shaughnessy R, Mahoney MG, et al. Desmoglein 4 in hair follicle differentiation and epidermal adhesion: evidence from inherited hypotrichosis and acquired pemphigus vulgaris. Cell 2003; 113: 249–260.
6. Kazantseva A, Goltsov A, Zinchenko R, Grigorenko AP, Abrukova AV, Moliaka YK, et al. Human hair growth deficiency is linked to a genetic defect in the phospholipase gene LIPH. Science 2006; 314: 982–985.
7. Pasternack SM, von Kugelgen I, Aboud KA, Lee YA, Ruschendorf F, Voss K, et al. G protein-coupled receptor P2RY5 and its ligand LPA are involved in maintenance of human hair growth. Nat Genet 2008; 40: 329–334.

Table I. *Features of genetic, non-syndromic human alopecias*

Disease (ref)	Hair shaft shape	Eyelash/eyebrow	Causative gene	Mode of inheritance
Hypotrichosis simplex of scalp (8)	Normal	Normal	*CDSN*	Autosomal dominant
Monilethrix (9)	Regularly spaced, spindle-shaped swellings	Absent to normal	*hHb1, 3, 6*	Autosomal dominant
Atrichia with papular lesions (10)	Normal	Absent	*HR*	Autosomal recessive
Hypotrichosis, Marie Unna type (11)	Iron-wire	Sparse	*U2HR*	Autosomal dominant
Hereditary hypotrichosis simplex (12)	Short, thin, easily plucked	Absent to sparse	*APCDD1*	Autosomal dominant
Localized hereditary hypotrichosis (LAH1) (2, 5, 13)	Moniliform	Absent to normal	*DSG4*	Autosomal recessive
Localized hereditary hypotrichosis (LAH2) (3, 6, 14)	Curled	Absent to normal	*LIPH*	Autosomal recessive
Localized hereditary hypotrichosis (LAH3) (4, 7, 15)	Curled	Absent to normal	*LPAR6*	Autosomal recessive

8. Davalos NO, Garicia-Vargas A, Pforr J, Davalos IP, Picos-Cardenas VJ, Garcia-Cruz D, et al. A non-sense mutation in the corneodesmosin gene in a Mexican family with hypotrichosis simplex of the scalp. Br J Dermatol 2005; 153: 1216–1219.
9. Richard G, Itin P, Lin JP, Bon A, Bale SJ. Evidence for genetic heterogeneity in monilethrix. J Invest Dermatol 1996; 107: 812–814.
10. Ahmad W, Faiyaz ul Haque M, Brancolini V, Tsou HC, ul Haque S, Lam H, et al. Alopecia universalis associated with a mutation in the human hairless gene. Science 1998; 279: 720–724.
11. Wen Y, Liu Y, Xu Y, Zhao Y, Hua R, Wang K, et al. Loss-of-function mutations of an inhibitory upstream ORF in the human hairless transcript cause Marie Unna hereditary hypotrichosis. Nat Genet 2009; 41: 228–233.
12. Shimomura Y, Agalliu D, Vonica A, Luria V, Wajid M, Baumer A, et al. APCDD1 is a novel Wnt inhibitor mutated in hereditary hypotrichosis simplex. Nature 2010; 464: 1043–1047.
13. Shimomura Y, Sakamoto F, Kariya N, Matsunaga K, Ito M. Mutations in the desmoglein 4 gene are associated with monilethrix-like congenital hypotrichosis. J Invest Dermatol 2006; 126: 1281–1285.
14. Horev L, Tosti A, Rosen I, Hershko K, Vincenzi C, Nanova K, et al. Mutations in lipase H cause autosomal recessive hypotrichosis simplex with wooly hair. J Am Acad Dermatol 2009; 61: 813–818.
15. Horev L, Saad-Edin B, Ingber A, Zlotogorski A. A novel deletion mutation in P2RY5/LPA_6 gene cause autosomal recessive woolly hair with hypotrichosis. J Eur Acad Dermatol Venereol 2010; 24: 858–859.

Clinics in Dermatology (2011) **29**, 412–419

ELSEVIER

Clinics in Dermatology

Ultrastructure and molecular pathogenesis of epidermolysis bullosa

Satoru Shinkuma, MD[a,*], James R. McMillan, MSc[b], Hiroshi Shimizu, MD[a]

[a]*Department of Dermatology, Hokkaido University Graduate School of Medicine, N15 W7, Sapporo 060-8638, Japan*
[b]*Centre for Children's Burns and Trauma Research, Queensland Children's Medical Research Institute, The University of Queensland, Brisbane, Queensland 4029, Australia*

Abstract Epidermolysis bullosa (EB) is classified into the three major subtypes depending on the level of skin cleavage within the epidermal keratinocyte or basement membrane zone. Tissue separation occurs within the intraepidermal cytoplasm of the basal keratinocyte, through the lamina lucida, or in sublamina densa regions of the basal lamina (basement membrane) in EB simplex, junctional EB, and dystrophic EB, respectively. Transmission electron microscopy (TEM) is an effective method for determining the level of tissue separation and hemidesmosome (HD) and anchoring fibril morphology if performed by experienced operators, and has proven to be a powerful technique for the diagnosis of new EB patients. Recent advances in genetic and immunofluorescence studies have enabled us to diagnose EB more easily and with greater accuracy. This contribution reviews TEM findings in the EB subtypes and discusses the importance of observations in the molecular morphology of HD and basement membrane associated structures.

Introduction

Epidermolysis bullosa (EB) comprises a group of hereditary disorders characterized by mechanical stress-induced blistering of the skin and mucous membranes.[1] This group of diseases is caused by a genetic abnormality in a single gene encoding one of 13 proteins involved in epidermal keratinocyte-basement membrane zone (BMZ) adhesion (Figure 1).[2,3] EB has typically been classified into three main subtypes, depending on the level of epidermal separation from the underlying basal lamina. Tissue separation occurs within the intraepidermal keratinocyte cytoplasm, through the lamina lucida, or in the sublamina densa in EB simplex (EBS), junctional EB (JEB), and dystrophic EB (DEB), respectively (Figure 2).[1] After the initial diagnosis based on careful examination of the clinical manifestations and inheritance pattern, a skin biopsy from a recently formed blister lesion should be taken to determine the level of tissue separation to classify the disease.[4]

Transmission electron microscopy (TEM) and immunofluorescence (IF) are both effective at determining the level of tissue separation.[5] Currently, IF is becoming increasingly important in the diagnosis of EB because TEM requires expensive equipment and significant experience and expertise to process skin biopsy specimens and accurately interpret the resulting micrographs.[4] The primary advantage of TEM, however, is that it can visualize ultrastructural abnormalities and provide a semiquantitative assessment of specific BMZ structural deficits.[6] Therefore TEM is likely to continue to assume an important role in both the clinical and research

* Corresponding author. Tel.: +81 11 716 1161x5962; fax: +81 11 706 7820l.
E-mail address: qxfjc346@ybb.ne.jp (S. Shinkuma).

0738-081X/$ – see front matter © 2011 Elsevier Inc. All rights reserved.
doi:10.1016/j.clindermatol.2011.01.010

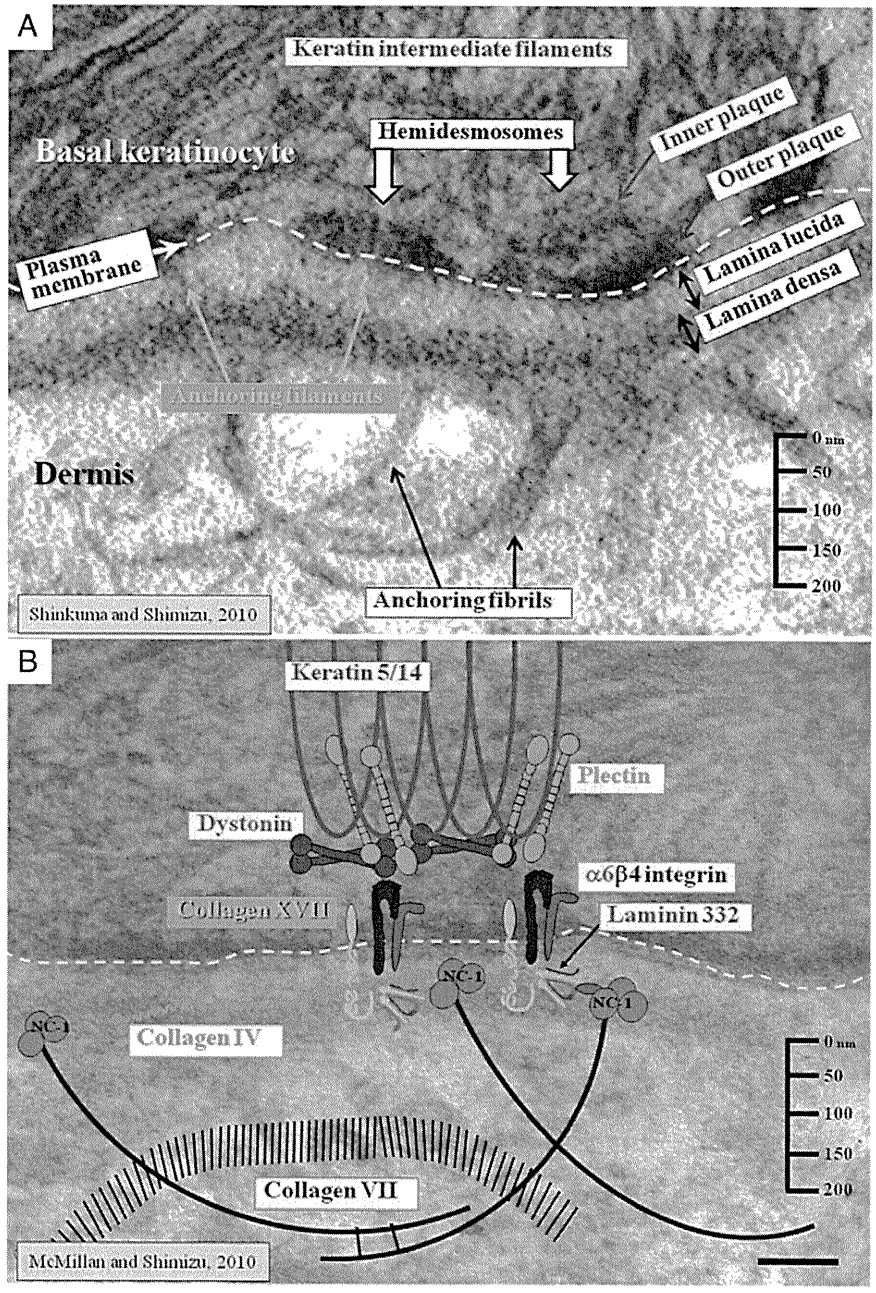

Fig. 1 Schematic diagram shows the approximate positions of principal epidermal basement membrane zone components. (Adapted with permission from McMillan et al.[3])

fields. This contribution focuses on TEM findings and their usefulness in EB diagnosis and cell adhesion research.

Ultrastructure of normal dermal–epidermal junction

The BMZ is composed of various molecules, each of which plays a differing role in dermal-epidermal junction adhesion (Figure 1).[3,7,8] The ultrastructural location of each BMZ molecule has been studied using a range of immunoelectron microscopy techniques.[7-9] In the basal keratinocyte, several electron dense rivetlike structures are found on the inner surface of the keratinocyte basal pole of the cell membrane, called hemidesmosomes (HDs).[10] HDs show a distinct tripartite, two-plaque structure, consisting of inner and outer plaques.[11-13] Keratin intermediate filaments (KIF), which are 10 to 12 mm thick and consist of basal cell keratins 5 and 14, associate with the inner hemidesmosome (HD) plaque and interplaque space and are capable of binding to both plectin and 230-kDa bullous pemphigoid